

SMC5 DEPLETION IMPEDES CELL CYCLE PROGRESSION,
INDUCES DNA DAMAGE, AND CAUSES GENOMIC INSTABILITY IN
MOUSE EMBRYONIC FIBROBLASTS

by
Himaja Gaddipati

A thesis submitted to Johns Hopkins University in conformity with the requirements for the
degree of Master of Science

Baltimore, Maryland

June 2015

Abstract

Introduction:

The structural maintenance of chromosomes 5/6 (Smc5/6) complex plays a critical role in maintaining genomic integrity. More specifically, Smc5/6 is involved in DNA replication, DNA damage repair via homologous recombination (HR), and chromosome segregation. Although its function has been extensively studied in yeast, few studies have evaluated Smc5/6 in mammalian models. Based on existing literature, we hypothesized that Smc5/6-deficient mouse embryonic fibroblasts (MEF) would accumulate DNA damage and, as a result, demonstrate abnormal mitotic progression and show evidence of replication stress.

Methods:

We used transgenic mice harboring a floxed exon 4 of the *Smc5* gene (*Smc5*^{flox/flox} and *Smc5*^{+/^{del}}, *Ert2-Cre*^{tg/0}) to breed and establish immortalized MEF cell lines with genotypes of *Smc5*^{flox/del}, *Ert2-Cre*^{tg/0} (experimental), *Smc5*^{+/^{flox}}, *Ert2-Cre*^{tg/0} (control #1), and *Smc5*^{flox/del} (control #2). *Smc5* exon 4 was deleted by addition of 0.2 μ M 4-OH tamoxifen for nine days. Deletion was confirmed by PCR and protein depletion by western blot. Cells were analyzed on day 3, 6 and 9.

MEF growth characteristics and cell cycle progression were evaluated by performing cell counts and FACS analysis, respectively. We also used immunofluorescence microscopy to observe micronuclei formation and DNA bridges. Additionally, we analyzed Rad51, Sumo1, and Sumo2/3 after treating cells with hydroxyurea. Finally, we used western blot analysis to evaluate expression of the stress response marker, p53.

Results:

Smc5-depleted MEFs demonstrated several mitotic abnormalities. After six days of 4-OH tamoxifen treatment, we observed a sustained, two-fold decrease in cell proliferation compared to controls. FACS analysis showed delayed entry into S-phase. DAPI staining of Smc5-depleted cells showed 12% increase in micronuclei formation and 33% increase in DNA bridges. Hydroxyurea-treated cells showed an accumulation of Rad51 foci, suggesting impaired HR mechanisms. Mutation of *Smc5* also resulted in a decline in Sumo1 but not Sumo2/3 foci. Lastly, western blot analysis showed significant p53 upregulation.

Conclusions:

For the first time, we have demonstrated the importance of the Smc5/6 complex in somatic mouse cells. Smc5 depletion in MEF cells compromises genomic integrity, affects cell cycle progression and leads to chromosome missegregation. We also demonstrate hypersensitivity to DNA damage agents and activation of the p53 pathway.

Advisor: Dr. Philip Jordan, Biochemistry and Molecular Biology

Thesis Reader: Dr. Janice Evans, Biochemistry and Molecular Biology

Acknowledgements

I would like to acknowledge the department of Biochemistry and Molecular Biology. My gratitude extends to the wonderful faculty and peers that have aided me in my studies. Special thanks to Dr. Barry Zirkin for his guidance on the MHS thesis, Dr. Marina Pyrzikova for teaching me all of the basic science laboratory skills I know to date, and Dr. Janice Evans for her extensive advising and support throughout my time here at Johns Hopkins University.

Lastly, I'd like to thank my ScM advisor, Dr. Philip Jordan. His infectious enthusiasm has forged a wonderful lab environment. I am forever grateful for his steadfast mentorship and the academic qualities he has instilled in me.

Table of Contents

Introduction	1-17
Structural maintenance of chromosome (SMC) proteins	1
SMC complex architecture	2-4
Mitotic role of SMC complexes	5-8
Smc5/6 and DNA damage repair via homologous recombination	9-11
Smc5/6 and chromosome segregation	12-13
Consequences of replication stress	14-16
Characterizing the effects of Smc5/6 depletion in mouse embryonic fibroblasts	17
Material and Methods	18-28
Mouse embryonic fibroblast (MEF) line derivation	18-19
Cell culture conditions	20
Polymerase chain reaction (PCR) analysis	20-21
Western blot analysis	21-22
Cell cycle analysis	23-24
MEF treatment schemes: cell synchronization and DNA damage agents	25-27
Immunofluorescence microscopy	28
Image acquisition and processing	28
Results	29-49
Conditional knockout of Smc5 in immortalized MEFs	29-32
Smc5 mutants exhibit decreased cell proliferation and aberrant mitosis	33-35
Smc5 mutants demonstrate delayed entry into S-phase of cell cycle	36-40
Smc5 depletion leads to p53 accumulation	41
Smc5-depleted cells demonstrate heightened sensitivity to hydroxyurea and etoposide	42-45
Hydroxyurea treatment leads to increased Rad51 accumulation in Smc5-depleted MEFs	46-47
Smc5 depletion leads to decline in SUMO1 but not SUMO2/3 in hydroxyurea treated cells	48-49
Discussion	50-54
Public health relevance	55-56
Supplemental figures	57-64
References	65-68
Resume	69-70

List of Figures

Figure 1: SMC complexes	5
Figure 2: SMC proteins during mitosis	8
Figure 3: Smc5/6-cohesin mediated HR repair	9
Figure 4: Smc5/6-mediated HR repair at stalled replication forks	12
Figure 5: Missegregation in Sm6 mutants	14
Figure 6: Replication stress-induced DNA damage	17
Figure 7: Mouse breeding scheme and cells lines	20
Figure 8: FACS analysis scheme	25
Figure 9: Nocodazole treatment scheme	26
Figure 10: Hydroxyurea treatment scheme	27
Figure 11: Etoposide treatment scheme	28
Figure 12: Smc5 knockout scheme	32
Figure 13: Confirmation of Smc5 knockout	33
Figure 14: Cell proliferation	35
Figure 15: Mitotic aberrancies	36
Figure 16: FACS analysis: control cell lines	39
Figure 17: FACS analysis: experimental cell lines	40
Figure 18: S-phase progression	41
Figure 19: p53 accumulation	43
Figure 20: Defects observed in hydroxyurea treated MEFs	45
Figure 21: Defects observed in etoposide treated MEFs	46
Figure 22: Rad51 accumulation in hydroxyurea treated MEFs	48
Figure 23: SUMO1 and SUMO2/3 accumulation in hydroxyurea treated MEFs	50
Supplemental Figure 1: FACS analysis of Experimental #1 untreated	56
Supplemental Figure 2: FACS analysis of Experimental #1 +4-OH TAM	57
Supplemental Figure 3: FACS analysis of Control #1 untreated	58
Supplemental Figure 4: FACS analysis of Control #1 +4-OH TAM	59
Supplemental Figure 5: FACS analysis of Experimental #2 untreated	60
Supplemental Figure 6: FACS analysis of Experimental #2 +4-OH TAM	61
Supplemental Figure 7: FACS analysis of Control #2 untreated	62
Supplemental Figure 8: FACS analysis of Control #2 +4-OH TAM	63

Introduction

Structural Maintenance of Chromosomes (SMC) proteins

The structural maintenance of chromosomes (SMC) proteins form a highly conserved group of complexes that play a key role in maintaining cell genomic integrity. SMC proteins are involved in essential chromosome-based processes, such as sister chromatid cohesion, chromosome condensation, and chromosome segregation. Additionally, SMC proteins have been found to play roles in DNA replication, DNA damage repair, and transcription (T. Hirano, 2006).

The SMC proteins interact with one another to form a V-like structure. In eukaryotes, there are six SMC members that form three heterodimeric protein complexes: cohesin (Smc1/3), condensin (Smc2/4), and Smc5/6 (Figure 1). Cohesin and condensin are known to be involved in two major cell division events: cohesion of sister chromatids, and pre-mitotic chromosome compaction, respectively. Mutations in either of these complexes results in dramatic disruption of chromosome segregation and causes genomic instability (Wu & Yu, 2012).

Unlike cohesin and condensin, the role of Smc5/6 is less well-defined. Though mechanistically unclear, studies in budding and fission yeast have shown Smc5/6 to be involved in double-strand DNA break (DSB) repair via homologous recombination (HR) (De Piccoli et al., 2006), maintenance of replication fork stalling (Irmisch et al., 2009), and chromosome segregation (Torres-Rosell et al., 2007). Smc5 and Smc6 mutants in budding yeast have been shown to accumulate X-shaped DNA structures. Investigated at different time points, these have been associated with both damaged replication forks (Branzei et al., 2006) and defective chromosome segregation (Tores-Rosell et al., 2005). Additionally, Smc5/6 mutants have demonstrated heightened sensitivity to DNA damage

agents, (reviewed in Stephan et al., 2011), further implicating its crucial role in DNA damage repair.

SMC complex architecture

The SMC proteins are made up of 1,000-1,500 amino acids and compile into structurally similar shapes. The N and C terminals contain Walker A and Walker B motifs, as well as half of an ATPase head. The protein folds in half, forming an intermolecular coiled coil that allows the ATPase halves to combine into a single globular head. On the opposite end, a hinge domain facilitates heterodimerization with another SMC protein. Smc1 pairs with Smc3 (cohesion), Smc2 pairs with Smc4 (condensin I and II), and Smc5 pairs with Smc6 (Potts, 2009).

Upon heterodimerization, an SMC complex is formed. Electron microscopy reveals that Smc1/3 and Smc2/4 can adopt several conformations, including V-shapes and ring-like structures (Hirano et al., 2001) (Figure 1 B). Dimerization also allows ATPase heads to interact with one another and hydrolyze ATP. Although similar in architecture, the sequences of Smc5 and Smc6 are divergent from Smc1-4 (Beasley et al., 2002).

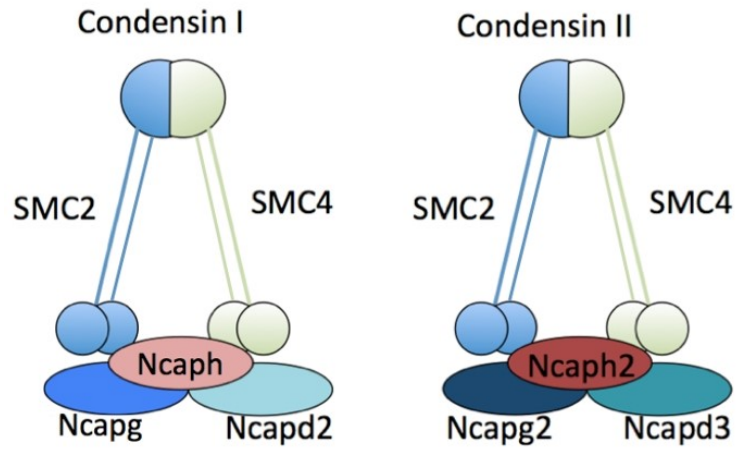
The SMC heterodimers also associate with other subunits to become a fully functional complex. Condensin has three subunits that interact with the head domain to complete the ring-like structure. Condensin I is comprised of proteins Ncaph, Ncapg and Ncapd2, while Condensin II interacts with Ncaph2, Ncapg2, and Ncapg3 (Wilson et al., 2013) (Figure 1 A). Similarly, Scc1 and Scc3 interact with the cohesin head domain to complete the loop. Smc5/6 has four non-SMC subunits that interact both transiently and

directly with the dimer. Nse1, Nse3, and Nse4 interact transiently with the head domain: Nse4 bridges the ATPase head, while Nse1 and Nse3 bind Nse4 and one another. Unlike these proteins, Nse2 (also known as Mms21) directly binds the arm of the Smc5 intermolecular coiled coil (Hirano, 2006) (De Piccoli et al., 2009) (Figure 1).

Nse1 and Nse2 have been shown to be essential for the function of Smc5/6. Mutations of Nse1 and Nse2 in fission yeast demonstrated phenotypes similar to the inactivation of the entire Smc5/6 complex (McDonald, Pavlova, Yates, & Boddy, 2003). Nse1 contains a RING domain with ubiquitin ligase activity, while Nse2 has a SP-RING domain with small ubiquitin-like modifier (SUMO) ligase activity (Potts, 2009). Sumoylation by Nse2 has been shown to be crucial for DNA damage repair (Wu and Kong et al., 2012), paralleling the overall implicated role of Smc5/6.

SMC complexes

A



B

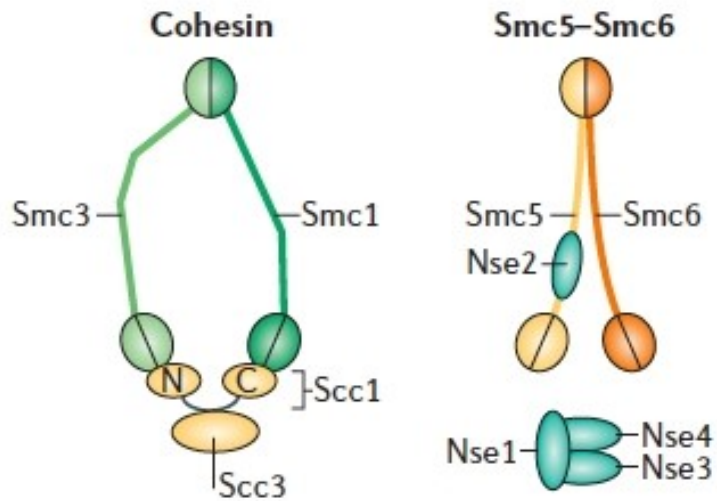


Figure 1 (A) Architecture of Condensin I and condensin II (W. Wilson & M, 2013) and (B) cohesin and Smc5/6 (Hirano, 2006).

Mitotic role of SMC complexes

The primary goal of mitosis is to accurately and completely duplicate genetic information and transmit DNA content to daughter cells. To ensure that this happens, the SMC proteins tightly regulate chromosome dynamics. At the onset of G1 phase, cohesin is activated by acetylation and recruited to establish sister chromatid cohesion during S-phase (Ben-Shahar et al., 2008). The ring structure of cohesin encircles the two sister chromatids and holds them together (Nasmyth, 2011). After replication, condensin II acts on chromosomes during prophase while condensin I is sequestered until prometaphase. Condensin II and condensin I are involved in axial shortening and lateral compaction, respectively, to resolve sister chromatids (Shintomi and Hirano, 2011). At the onset of condensin II loading, cohesin is simultaneously released further promoting chromatid resolution by weakening physical linkages. At anaphase, cohesin is completely released by separase-induced cleavage of the kleisin subunit, Scc1. A balancing act between condensin II, condensin I and cohesin is needed for successful chromosome segregation (T. Hirano, 2015) (Figure 2).

Unlike cohesin and condensin, the role of Smc5/6 is less distinct. Smc5/6 plays a role from S-phase through M-phase, and is involved in both DNA damage repair and non-repair functions. During S-phase, Smc5/6 ensures faithful replication by promoting HR-mediated repair of DNA damage, but also avoiding complex recombination intermediates (reviewed in Murray and Carr, 2008). HR repair is essential for the repair of stalled replication forks and DSBs from yeast to mammals (Saleh-Gohari et al., 2005).

Cohesin loading at the site of DNA damage is thought to promote HR by holding sister chromatids in close proximity to each other (Strom et al., 2007). DNA damage

activates the protein kinases ataxia telangiectasia and Rad3-related protein (ATR) and Checkpoint kinase 1 (Chk1), initiating a signal transduction pathway (Smith et al., 2010). In budding yeast, ATR/Chk1 phosphorylates the cohesin subunit, Scc1 (Heidinger-Pauli et al., 2009). In turn, establishment of cohesin 1 (Eco1), an acetyltransferase that is needed for sister chromatid cohesion (Ivanov et al., 2002), also modifies Scc1 via acetylation (Heidinger-Pauli et al., 2009). This antagonizes the wings apart-like (Wapl) protein, which normally binds to cohesin and facilitates cohesin removal from chromosome arms (Gandhi et al., 2006). Thus, displacement of Wapl promotes cohesin loading at the site of DNA damage (Unal et al., 2007).

Though the mechanism is unknown, Smc5/6 is needed to maintain cohesin at DNA lesions (De Piccoli et al., 2006; Strom et al., 2007). In budding yeast, Smc5/6 is recruited by the repair factor Mre11, which accumulates early on at the site of DNA damage (Lindross., Strom, 2006). In human cells, Smc5/6 was shown to modulate HR via sumoylation of Scc1 by Nse2 (Wu and Kong et al, 2012) (Figure 3).

In line with a role in DNA damage repair, chromatin immunoprecipitation (ChIP)-on-chip analysis of chromosome XII in budding yeast showed that Smc6 accumulates at DSBs and stalled replication forks (Nasmyth, 2011). Additionally, Smc5/6 was shown to accumulate at centromeric regions during the G2/M-phase in undamaged cells, suggesting it plays a role in chromosome segregation (Lindross et al., 2006). During replication and HR repair, joint molecules, physical attachments, and sister chromatid intertwining can develop, creating a topological stress for cells. If not relieved, chromosome segregation is blocked (Murray et al., 2008; Jeppsson et al., 2014). In budding yeast, sister chromatid intertwining is resolved by Topoisomerase II (Top2). In

Top2 mutant yeast cells, Smc5/6 bound to chromosomes in a cohesin-dependent manner. The amount of Smc5/6 on chromosome arms was positively correlated with missegregation events, suggesting that Smc5/6 is needed for accurate chromosome segregation (Jeppsson et al., 2014).

SMC proteins during mitosis

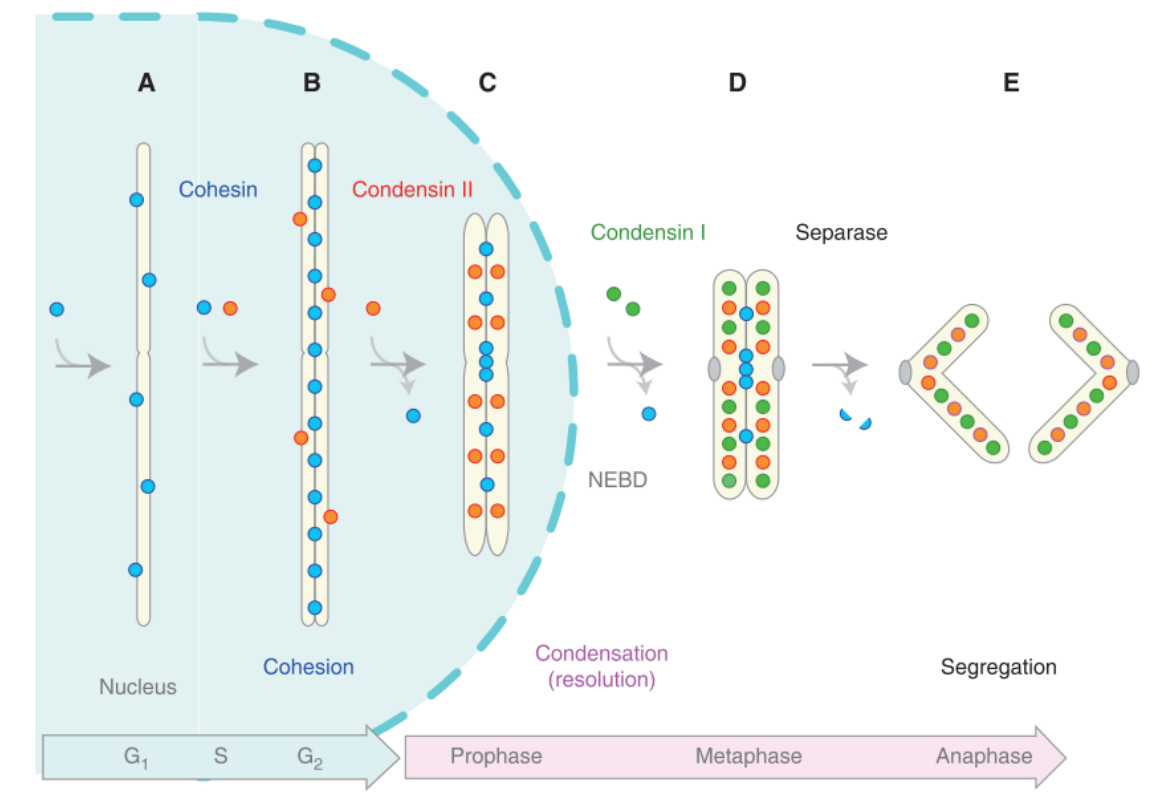


Figure 2 Interplay of cohesin, condensin II, and condensin I during mitosis (Hirano, 2015).

Smc5/6-cohesin mediated HR repair

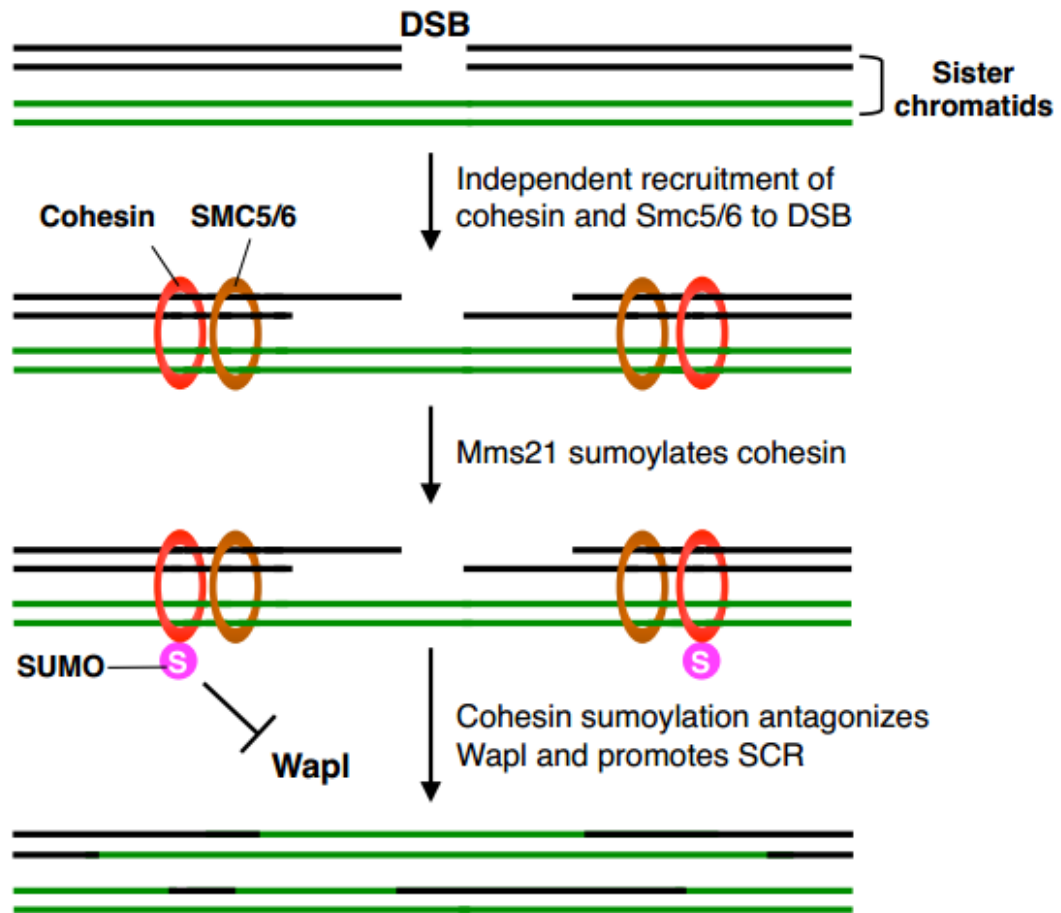


Figure 3 Model of Smc5/6 and cohesin involvement in HR-mediated repair of DSBs (Wu and Kong et al., 2012).

Smc5/6 and DNA damage repair via homologous recombination

Several studies have associated Smc5/6 with homologous recombination. Induction of DNA damage using various agents (ionizing radiation, ultraviolet radiation, methyl methanesulfonate, hydroxyurea and etoposide) have shown an increase in mitotic catastrophe among Smc5/6 mutants (Wu and Yu, 2012). Three common substrates of homologous recombination have been studied: DSBs, stalled replication forks, and collapsed replication forks. Repair of all three substrates is essential as they threaten cell viability and genomic integrity. DSBs are among the most serious types of DNA damage as they can lead to lethality. Prolonged replication fork stalling and collapse can also lead to DSBs (Saleh-Gohari et al., 2005).

Smc6 was shown to localize to DSBs during the G2 and M-phase (Piccoli et al., 2006, Lindross et al., 2006). Two primary types of repair mechanisms are employed to repair DSBs: non-homologous end joining (NHEJ) and HR. De Piccoli et al reported that budding yeast Smc5/6 mutants showed a four-fold decrease in DSB repair and a 100-fold increase in gross chromosomal arrangements. However, NHEJ repair was not affected, suggesting that Smc5/6 plays an exclusive role in mediating HR (De Piccoli et al., 2006).

Homologous recombination is considered to be an error-free method of repairing DNA damage. The HR pathways uses the exchange of a similar DNA sequence, such as a sister chromatid, as a template for repair. Strand invasion of the ssDNA is mediated by Rad51, forming a characteristic D-loop (Li & Heyer, 2008). In fission yeast, two time-dependent HR models were proposed for resolving stalled replication forks. During early replication fork stalling, Smc5/6 maintains stalled forks in a recombination-competent

conformation in order to prime forks for restart. During late replication fork stalling, Smc5/6 mediates resolution of DNA structures (Irmisch et al., 2009). Alternatively, DNA damage can also be bypassed via a HR-dependent template switch mechanism (reviewed in Kegel et al., 2011) (Figure 4).

Although the role of the Smc5/6 complex during HR is still mechanistically unclear, ongoing studies are providing insights into how it may be working. First, Roy et al. showed that Smc5 and Smc6 have a higher binding affinity for ssDNA than dsDNA. This is an important observation because ssDNA accumulates at the initial stages of replication fork stalling or DNA damage. The ability of Smc5/6 to bind even small sections of ssDNA (~60nt), supports the idea that Smc5/6 mediates HR repair (Roy and D'Amours et al., 2011; Roy and Siddiqui et al., 2011). Furthermore, Smc5/6 was shown to bind synthetic DNA molecules that were designed to resemble structures created during HR. Smc5/6 efficiently bound to synthetic Holliday junctions and splayed Y models, suggesting that Smc5/6 plays a direct role in HR (Roy et al., 2015).

Additionally, Nse2-deficient budding yeast were shown to accumulate X-shaped DNA structures at stalled replication forks. Because these accumulated in a Rad51 dependent manner, the DNA structures are thought to be HR intermediates (Branzi et al., 2006). Similarly, IR-induced DSBs in *Drosophila melanogaster* heterochromatin were shown to use HR repair. Smc5/6 was found to be physically associated with HP1a, a histone modification protein that is enriched in heterochromatin. DNA repair sites were shown to expand and re-localize outside of the HP1a domain, where they associate with Rad51. Smc5/6 recruitment was shown to preclude Rad51 formation, suggesting that Smc5/6 promotes exclusion of Rad51 foci so that recombination can occur outside of

heterochromatin (Chiolo et al., 2011). HR within heterochromatin can cause loss or duplication of information due to the large number of repeat sequences (Peng et al., 2008). In further support of this model, Smc5/6 depletion caused an accumulation of Rad51 within heterochromatin (Chiolo et al., 2011).

Smc5/6-mediated HR repair at stalled replication forks

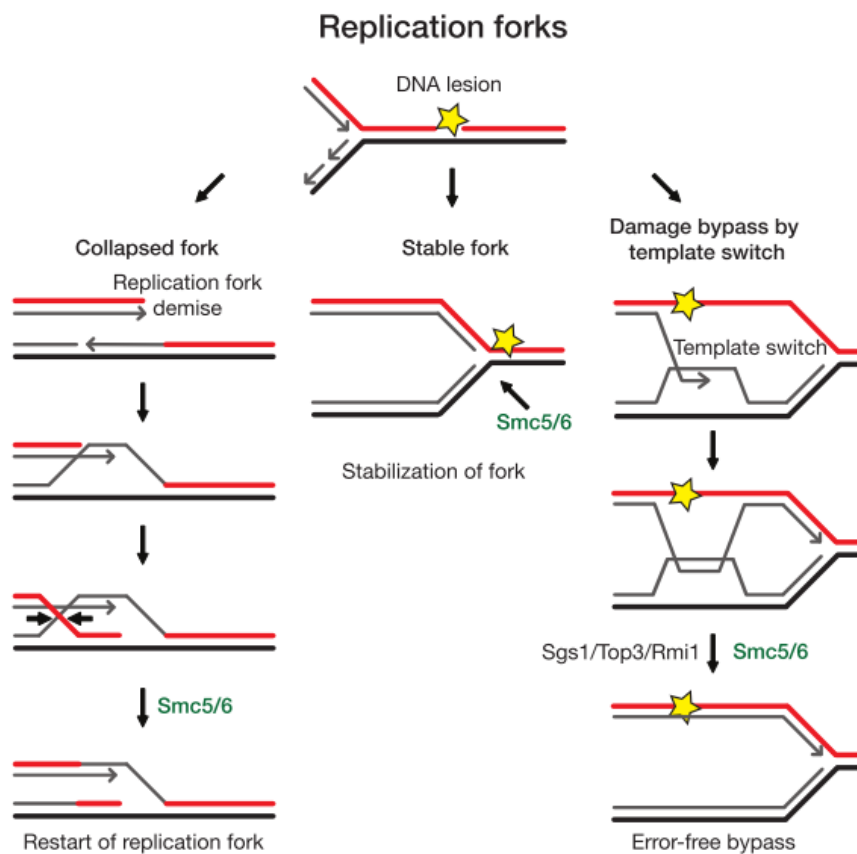


Figure 4 Proposed roles for the Smc5/6 complex during HR at stalled replication forks. At the onset of DNA lesions, Smc5/6 is involved in mediating replication fork restart, replication fork stabilization, or lesion bypass via template switching (Kegel et al., 2015)

Smc5/6 and chromosome segregation

In addition to HR-mediated repair, Smc5/6 has been proposed to play an active role in chromosome segregation. Post-HR, sister chromatids are held together by joint molecules that need to be removed for accurate chromosome segregation. If not removed in a timely fashion, aberrant chromosome rearrangement and breakage can occur during cell division. Smc6 mutants in budding yeast were shown to accumulate sister chromatid junctions. Upon reactivation of Smc6, junctions were dissolved (Bermudez-Lopez et al., 2010). Similarly, *NSE2* mutant human cells were shown to be hypersensitive to UV exposure, and accumulated sister chromatid exchanges (Payne et al., 2014).

A segregation analysis of chromosome XII in budding yeast showed evidence of unequal division of centromeres in Smc5/6 mutants. It was suggested that unresolved linkages enriched at the centromeric regions lead to chromosome nondisjunction (Torres-Rosell et al., 2007) (Figure 5). Chromosome missegregation has also been observed in human cells. Staining with CREST, a kinetochore marker, showed unequal centromere division in Smc5/6 mutant daughter cells. Additionally, DAPI staining and immunostaining for BLM and PICH revealed lagging chromosomes and DNA bridges (Gallego-Paez et al., 2013).

Lastly, mitotic failure in fission yeast Smc5/6 mutants has also been associated with sustained cohesin on chromosome arms. Cohesin localization was analyzed by ChIP using Rad21-GFP in hydroxyurea-treated cells. Wild-type cells showed loss of cohesin once cells went through mitosis. Smc6 mutants, however, showed retention of cohesin on

chromosome arms. Although cells still passed through anaphase, about three-quarters of cells did not become viable during the following G1 phase due to chromosomes being cut or incompletely resolved. Outwin et al. propose that the Smc5/6 complex affects chromosome dynamics by interacting with cohesin in either a direct or indirect way (Outwin et al, 2009).

Missegregation in Smc6 mutants

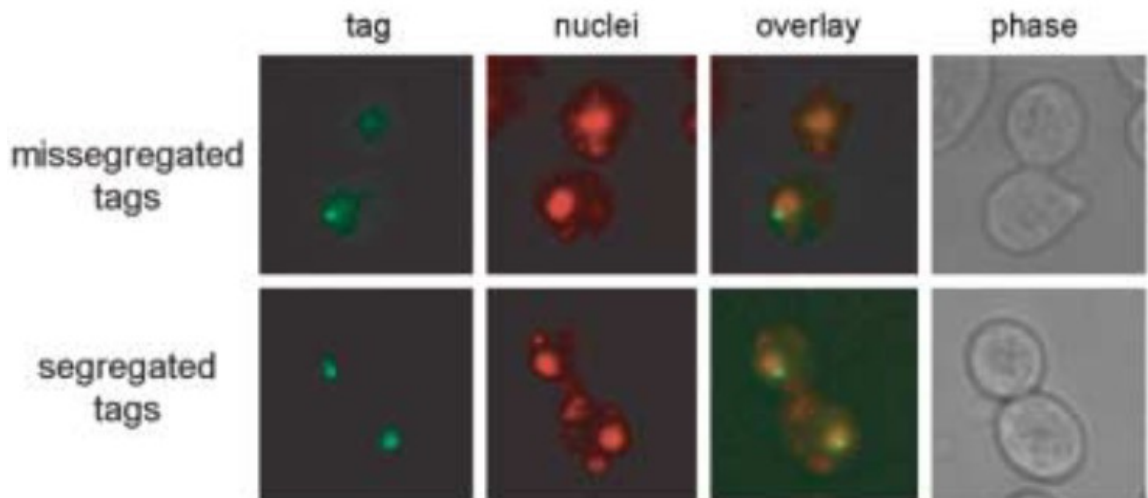


Figure 5 Smc6 mutant cells from budding yeast with DNA-based tags (Torres-Rosell et al., 2007).

Consequences of replication stress in Smc5/6 mutants

Correlating with the requirement of Smc5/6 during HR-mediated repair and chromosome segregation, Smc5/6 mutants from yeast to man show robust evidence of replication stress. DNA damage during S-phase and G2 phase leads to checkpoint arrest that is stimulated by two kinases, Ataxia telangiectasia mutated (ATM) and ataxia telangiectasia and Rad3-related protein (ATR). ATM/ATR signaling is necessary to mediate DNA repair and reentry into mitosis (Shiloh, 2003). In budding yeast, ATR is the main checkpoint response that modulates S-phase progression. Under genotoxic stress, ATR delays replication origin firing, and leads to delayed S-phase entry (Putnam et al., 2009). Smc6 mutants showed an ATR-dependent S-phase delay (Chen et al., 2013). Additionally, Nse2 was shown to be phosphorylated by ATR at serine 260 and 261, suggesting that ATR activation regulates Nse2-dependent DNA repair mechanisms (Carlborg et al., 2015).

At the onset of DNA damage, ATR regulates another protein kinase, Chk1, which is essential for the G2/M damage checkpoint (Lui et al., 2000). In turn, Chk1 has been identified as one of the many proteins that can modify and regulate the tumor suppressor protein, p53 in response to DNA damage. p53 plays a major role in preserving genomic integrity by mediating stress-induced growth arrest or senescence (Ou et al., 2005). In human and mouse fibroblasts, p53 was shown to contribute to a checkpoint that ensures DNA is completely replicated before progressing into M-phase. Overexpression of p53 inhibited mitotic entry even when cells were not stressed, suggesting that p53 modulates cell cycle progression (Taylor et al., 1999). To our knowledge, p53 has not been assessed in Smc5/6 mutants. However, given the widespread roles of p53 and evidence of

ATR/Chk1 activity in Smc5/6 mutants, it is plausible that p53 is also being activated upon replication stress.

In addition to altering signaling cascades, replication stress can also manifest as a cell shape deformity. Unreplicated, intertwined, or tangled DNA can lead to the formation of anaphase bridges. Two types of DNA bridges have been noted in mammalian cells. One can be visualized by DAPI staining and is induced by HR-defective cells. The other type, known as ultrafine bridges, cannot be detected by DAPI. However, they can be immunostained for proteins involved in resolving bridge structures, such as PICH and BLM (Gelot et al., 2015). Both types of bridges have been found in Smc5/6 deficient cells (Gallego-Paez et al., 2014) (Figure 6 A, B).

Replication stress can also be transmitted to daughter cells. After cytokinesis, the formation of micronuclei has been observed (Figure 6 C). Micronuclei are aggregates of lagging chromosomes, acentric chromosomes, and chromatid fragments that are enveloped in their own nuclear membrane. Micronuclei can persist over several generations and undergo asynchronous replication (Gelot et al., 2015). Human cells deficient in proteins that resolve DNA bridges, such as FANCM and BLM, have shown a higher rate of micronuclei formation. Human cells deficient in NSE2 function have also shown a similar trend (Payne et al., 2014).

Replication stress-induced DNA damage

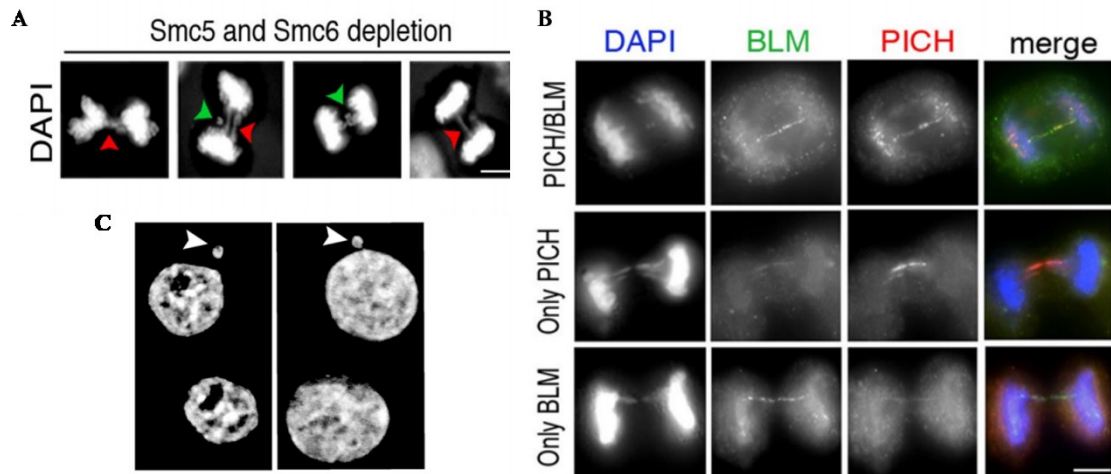


Figure 6 Examples of (A) DAPI stained bridges, (B) ultrafine bridges (Gallego-Paez, Tanaka et al., 2014) and (C) micronuclei (Payne et al., 2014) in Smc5/6 depleted human cells.

Characterizing the effects of Smc5/6 depletion in mouse embryonic fibroblasts

Thus far, Smc5/6 has largely been studied in lower organisms. In this study, we aimed to describe the role of Smc5/6 during mitosis in somatic mouse cells. We used a conditional knockout of *Smc5* to characterize defects in immortalized mouse embryonic fibroblasts (MEF). Based on the implicated roles of the Smc5/6 complex during DNA damage repair and chromosome segregation, we hypothesized that Smc5/6 mutants would demonstrate multiple abnormalities during the cell cycle. We show evidence of replication stress via cell growth patterns, cell cycle analysis, immunostaining, and detection of elevated p53 levels. Additionally, we studied Rad51 accumulation and SUMO patterns in hydroxyurea-treated cells.

Materials and Methods

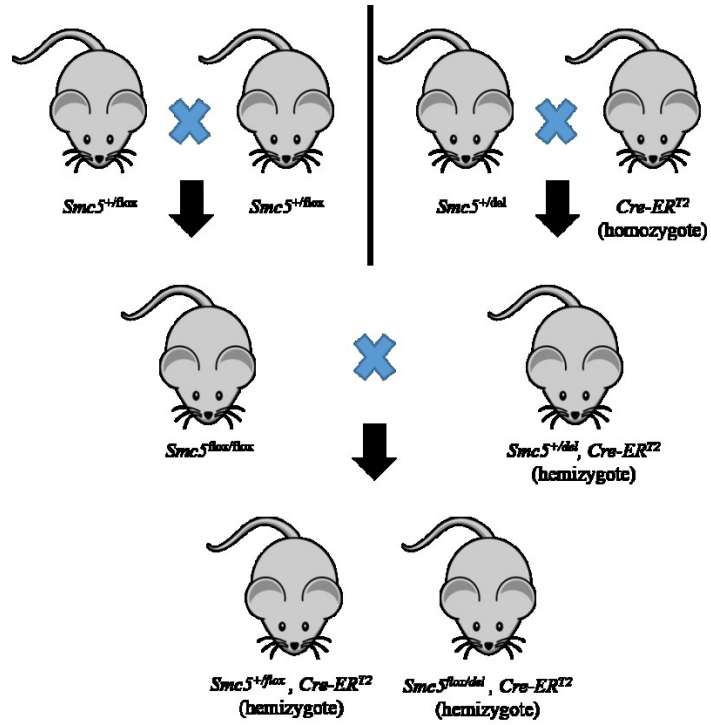
Mouse embryonic fibroblast (MEF) line derivation

Heterozygous mice ($Smc5^{+/del}$) were bred with mice homozygous for $Cre-ER^{T2}$ to acquire the Cre recombinase transgene. Additionally, mice heterozygous for the flox allele ($Smc5^{+/flox}$) were bred to obtain mice homozygous for the flox allele ($Smc5^{flox/flox}$). Progeny of these mice were bred to obtain hemizygous $Cre-ER^{T2}$ fetuses with $Smc5^{flox/del}$ (experimental) and $Smc5^{+/flox}$ (control #1) genotypes. 13.5 dpc fetuses with these genotypes were used to establish MEF lines. In addition, $Smc5^{flox/del}$ mice without the $Cre-ER^{T2}$ transgene (control #2) were used to establish an additional control line (Figure 7).

For long-term studies, MEFs were immortalized according to the NIH-3T3 protocol (Todaro et al., 1963). Primary mouse cells were passaged every three days until cells entered senescence. MEFs were monitored for regrowth and passaged until cells resumed a stable growth pattern (passage ~10-15). Cells were stored in liquid nitrogen in freezing medium (20% fetal bovine serum (FBS) (HyClone), 10% DMSO (Sigma), and 70% cell culture medium).

Mouse breeding scheme and cells lines

A



B

<u>Experimental #1 + #2</u>	<u>Control #1</u>	<u>Control #2</u>
$Smc5^{flox/del}, Cre-ER^{T2}$	$Smc5^{+/flox}, Cre-ER^{T2}$	$Smc5^{flox/del}$

Figure 7 (A) Mouse breeding scheme. (B) Genotypes of cell lines.

Cell culture conditions

MEFs were cultured in DMEM (Invitrogen) supplemented with 10% FBS (Hyclone) and penicillin-streptomycin (100U/mL and 100 μ g/mL) (Invitrogen). After thawing, cell growth was monitored for resumption of normal growth. MEFs took about 3-5 days to achieve 80-90% confluency. Once cells became sub-confluent, MEFs were passaged every three days. Cells were washed twice with PBS (Invitrogen), and then treated with 0.05% trypsin-EDTA for 2-3 minutes for detachment. After neutralizing trypsin-EDTA with cell culture medium, cells were counted using a hemocytometer and replated at a density of 10,000 cells/cm².

The deletion in *Smc5* gene was induced by treating experimental cells with 0.2 μ M 4-OH tamoxifen (Sigma H7904) (4-OH TAM). 4-OH TAM in cell culture medium was replenished every 2 days. MEFs were collected after 3, 6, and 9 days of 4-OH TAM treatment. Samples were washed with PBS, snap-frozen, and stored at -80°C for further analysis.

Polymerase chain reaction (PCR) analysis

DNA was extracted using the Thermo Scientific GeneJet Genomic DNA purification kit. DNA concentration was measured using Nano-Drop (Fisher Scientific). 50ng of DNA was used for each cell sample. Each PCR reaction contained a total volume of 50 μ L, consisting of 1x Taq polymerase buffer (5 Prime), 0.1mM dNTPs (5 Prime), 2.5U Taq polymerase (5 Prime), and 0.1 μ M of each primer (Integrated DNA Technologies) in milli-Q water.

To assess genotypes, primer pairs **93** 5'-ACTCAGTCTCACACGGCAAG-3' (forward) and **83** 5'-AGAAAGACATCAAATAACCGCTGGC-3' (reverse) were used to amplify wild type (410bp) and del (763bp) band fragments. For loxP sites, primer pairs **93** (forward) and **94** 5'-ATCCTTCCCACCTTGGAAAC-3' (reverse) and **83** (reverse) and **84** 5'-GAGATGGCGCAACGCAATTAAT-3' (forward) were used. Product sizes were 563bp and 644bp respectively.

The following PCR conditions were used:

1. Denaturation: 90°C for 1 min.
2. Denaturation: 90°C for 20 seconds.
3. Annealing: 58°C for 30 seconds.
4. Amplification: 72°C for 1 minute.
5. Steps 2-4 were repeated for 30 cycles.
6. Final extension: 72°C for 10 minutes.

After completion of PCR reaction, 20µL of each sample were resolved in 1.5% agarose gel.

Western blot analysis

Protein was extracted from cell samples by lysing 20,000 cells per 1µL of RIPA buffer (Santa Cruz) with 1x protease inhibitor (Roche) and 1x PhosSTOP phosphatase inhibitor (Roche). To remove cell debris, protein lysates were sonicated (Bioruptor sonication system) at high intensity for 5 minutes with 30 second on/off intervals, and centrifuged at 10,000 rpm for 10 minutes. The supernatant was transferred into a fresh

tube and pellet was discarded. Protein concentration was measured using BCA assay kit (Pierce). 30µg of protein were used for analysis. Prior to loading, samples with added Laemmli buffer (Bio-Rad) were boiled at 95°C for five minutes.

For Smc5 and Smc6 protein detection we used 6.5% polyacrylamide homemade gels (Sambrook et al., 2001). For p53, 4-15% polyacrylamide gradient gel (Bio-Rad) was used. All gels were run at 100V to resolve proteins. Proteins were transferred from gels onto a PVDF membrane (Bio-Rad) using TransBlot turbo system (Bio-Rad). After transfer, membranes were blocked in 3% bovine serum albumin (BSA) in PBS overnight.

Primary antibodies were diluted in 3% BSA in PBS: rabbit anti-Smc5 (Bethyl, A300-236A) 1:400, rabbit anti-Smc6 (Abcam, ab155495) 1:400, rabbit anti-p53 (Santa Cruz, 6243) 1:200, rabbit anti-Acetyl-p53 (Cell Signaling, 2570) 1:1000, and mouse anti- α -tubulin (Sigma, T9026) 1:20,000. Secondary horseradish peroxidase conjugated-antibodies goat anti-rabbit (Invitrogen, A10533) or rabbit anti-mouse (Invitrogen, R21455) were diluted 1:4000 in PBS.

Membranes were incubated with primary antibody for 1 hour, followed by two 15 minute washes in rinse buffer (PBS + 0.1% Tween-20). Subsequently, secondary antibodies conjugated to horse radish peroxidase were added for 1 hour, followed by one 15 minute wash and two 5 minute washes in rinse buffer. After final 5 minute wash in PBS, ECL (Thermo Scientific) was added to membranes in the dark for 1-2 minutes. Membranes were immediately imaged using Syngene XR5 system.

Cell cycle analysis

MEFs were plated at a density of 10,000 cells/cm² onto tissue culture vessels and treated with 0.2μM 4-OH TAM for a total of 6 days. On Day 4 of 4-OH TAM treatment, cells were switched to low-serum medium (0.5% FBS) for 48 hours to induce cell cycle arrest in the G0/G1 phase. After washing once with PBS, cells were released from serum starvation by addition of regular cell culture medium (10% FBS). Cells were collected at 0, 12, 15, 18, 21, and 24 hours after release (Figure 8). Collected cells were fixed by adding 3mL of 100% cold ethanol drop by drop to cell suspension in 1ml PBS. Cells were stored at -20°C.

Twenty four hours before cell cycle analysis fixed MEFs were washed twice in 4mL of cold PBS and centrifuged at 400g for 10 minutes. Cell pellet was resuspended in 1mL of staining solution (PBS with 0.1% Triton X-100, 0.2mg/mL RNase A, and 20μg/mL propioid iodide). Cells were kept at 4°C in the dark overnight.

FACS analysis scheme

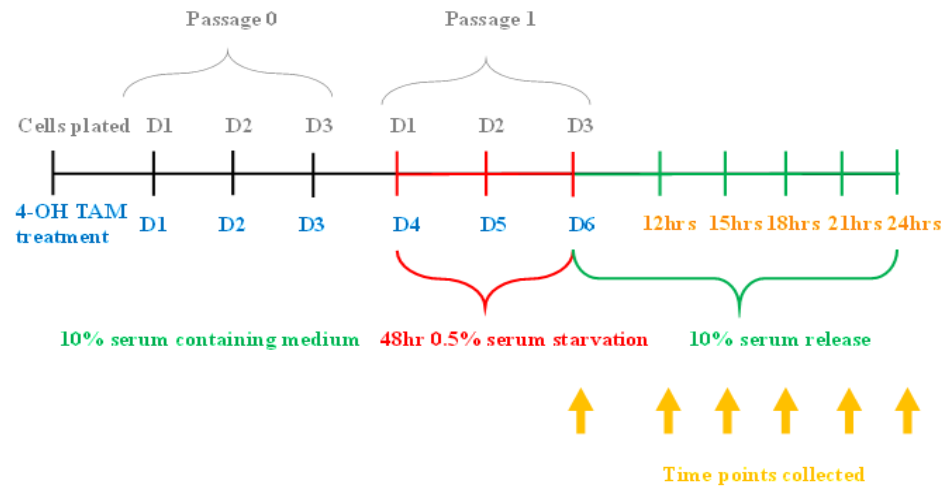


Figure 8 Cell synchronization scheme used for FACS analysis.

MEF treatment schemes: cell synchronization and DNA damage agents

MEFs were grown in cell culture vessel for 4 days and then plated onto sterile glass coverslips coated with 0.1% gelatin (Sigma). On Day 5, cells were treated according to the schemes below. Experimental MEFs were maintained in 0.2 μ M 4-OH TAM for the duration of the experiment. All cells were fixed with 10% formalin (Sigma) for 20 minutes at room temperature (RT), washed twice with PBS and stored at 4°C in PBS.

Nocodazole

To observe anaphases, MEFs were synchronized in G2 phase of cell cycle using nocodazole (Cayman). Cells were treated with 0.1 μ g of nocodazole for 24 hours. After washing once with PBS, cells were released in nocodazole-free medium and fixed after 45 minutes (Figure 9).

Nocodazole treatment scheme

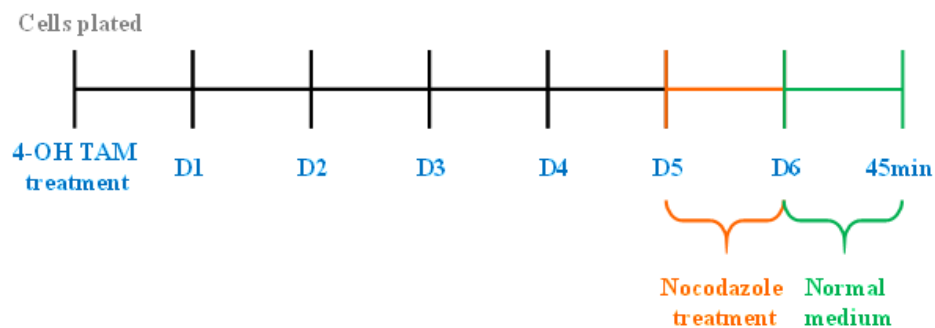


Figure 9 Cells were synchronized in G2 phase using nocodazole.

Hydroxyurea

Replication fork stalling was induced by treating cells with 2mM hydroxyurea (HU) (Sigma) for 24 hours. Following HU treatment, cells were synchronized in G2 phase using 0.1 μ g nocodazole for 24 hours. Cells were released in normal medium and fixed after 45 minutes to observe mitotic recovery and cell cycle progression (Figure 10).

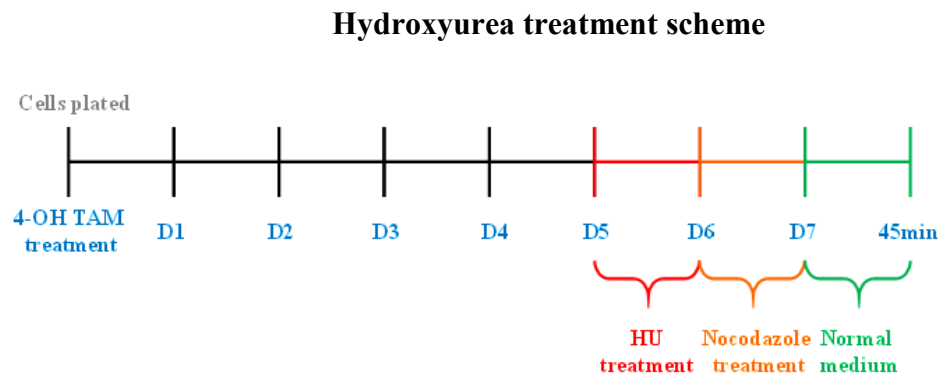


Figure 10 Scheme for hydroxyurea treatment

Etoposide

Cells were treated for 6 days with 0.2 μ M 4-OH TAM, followed by 24 hours with 0.1 μ g nocodazole. Cells were released in normal medium for 2 hours to allow entry into mitosis. After entry, cells were treated with 15mM etoposide (Sigma) for 12 hours to block topoisomerase II activity and induce double strand breaks. After etoposide treatment, MEFs were released in normal medium for 12 hours to observe DNA damage recovery (Figure 11).

Etoposide treatment scheme

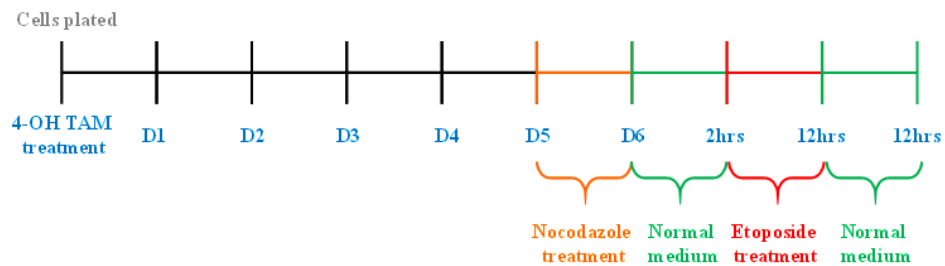


Figure 11 Scheme for etoposide treatment

Immunofluorescence microscopy

Prior to antibody staining, fixed cells were permeabilized with 0.1% Triton X-100 (Sigma) for 10 minutes at RT, washed once in TBST (Sigma) wash buffer and blocked with 4% horse serum in PBS for 30 minutes at RT. Incubation with primary antibody was performed for 1 hour at RT, followed by 3 washes. Secondary antibodies conjugated with fluorophore were added for 1 hour in the dark. After 3 washes in the dark, cells were mounted onto super frosted microscope slides (Fisher) using mounting medium with DAPI (Vector Labs).

Primary antibodies are as follows: rabbit anti-Rad51 (Thermo, PA527195) 1:100, mouse anti-SUMO1 (Matunis et al., 1996) 1:500, mouse anti-SUMO2/3 (Zhang et al., 2008) 1:200, human anti-centromere (Antibodies incorporated, 15-235) 1:50, and mouse anti- α -tubulin (Sigma, T9026) 1:1000. Secondary antibodies raised against rabbit, mouse and human IgG and conjugated to Alexa 488, 568, and 633 (Life Technologies) were used at 1:3000 dilution.

Image acquisition and processing

Images were acquired using Zeiss Cell Observer Z1 linked to an ORCA-Flash 4.0 CMOS camera (Hamamatsu) and analyzed with the Zeiss ZEN 2012 blue edition image software. Z stacks were acquired at 40x magnification with a region of interest (ROI) of 512x512 pixels. Original images were processed by deconvolution for better clarity, and then a single image, which combined in focus light from each stack, was created using variance-based extended depth focusing. RAD51, SUMO1, and SUMO2/3 foci were counted using ImageJ by processing for image maxima. Photoshop (Adobe) was used to prepare figures.

Results

Conditional knockout of *Smc5* in immortalized MEFs

A Cre-flox system was used to obtain four MEF lines with the following genotypes: *Smc5^{flox/del}*, *Cre-ER^{T2}* (Experimental #1 and #2), *Smc5^{+flox} Cre-ER^{T2}* (Control #1) and *Smc5^{+flox}* (Control #2). The *Smc5* flox allele contains two loxP sites surrounding exon 4, while del allele has exon 4 deleted (Figure 12 A). The Cre-ER^{T2} recombinase was used to induce recombination between the loxP sequences, leading to excision of *Smc5* exon 4 (Figure 12 B). Exon 4 was chosen as a target because it has been identified in all *Smc5* transcripts. Additionally, the floxed exon is the 4th of 23, and is located early within the open reading frame. Therefore the mutation is likely to produce an unstable transcript, not capable of facilitating protein synthesis or a stable polypeptide. To induce Cre-ER^{T2} recombinase expression, 0.2μM of 4-OH TAM was added to cell culture medium for 3, 6 and 9 days.

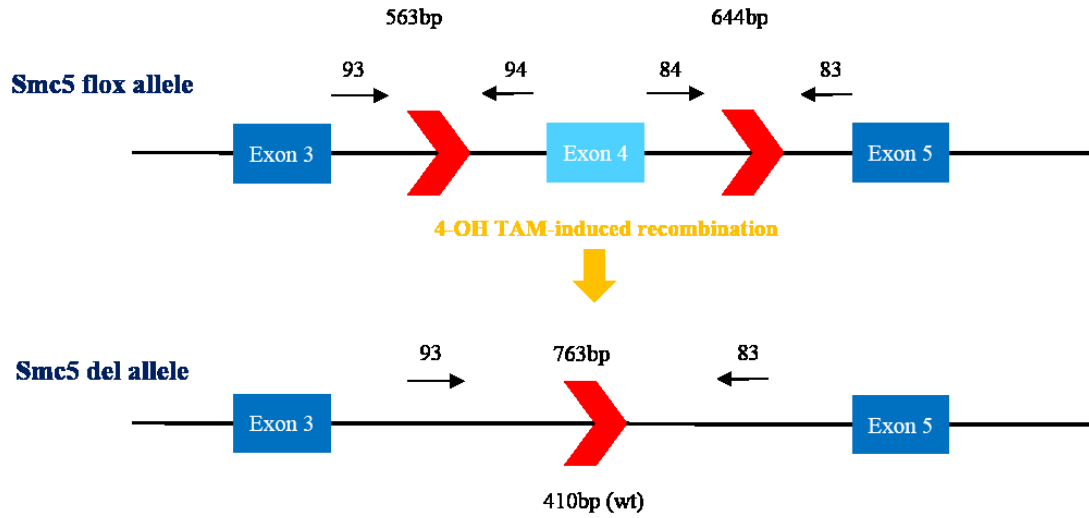
Deletion of exon 4 was confirmed by PCR. Primers pairs 93, 94, and 83, 84 detected flox alleles with product sizes of 563bp and 644bp, respectively. Primers 93 and 83 were used to detect del and wild type alleles with product sizes of 763bp and 410bp, respectively (Figure 12 A). Experimental lines showed a substantial decrease in flox alleles and an increase in del allele by Day 6. Control lines also showed a decrease in flox alleles while maintaining the wild type allele. Deletion was more efficient in control lines (Figure 13 A).

Analogous to PCR results, western blot analysis showed partial depletion of Smc5 and Smc6 by Day 3, and complete protein depletion by Day 9 (Figure 13 B). Decline in Smc6 protein levels supports the idea that Smc5 and Smc6 function as a complex, rather

than as individual proteins. In the control line, we observed variable protein depletion after 9 days of 4-OH TAM treatment. It is possible that heterozygosity is causing a decline in protein levels. However, mice heterozygous for the *Smc5* delete allele do not display any abnormal phenotypes, leading us to believe that this difference is insignificant. To further bypass this issue, we conducted all of our experiments after 6 days of 4-OH TAM treatment.

Smc5 knockout scheme

A



B

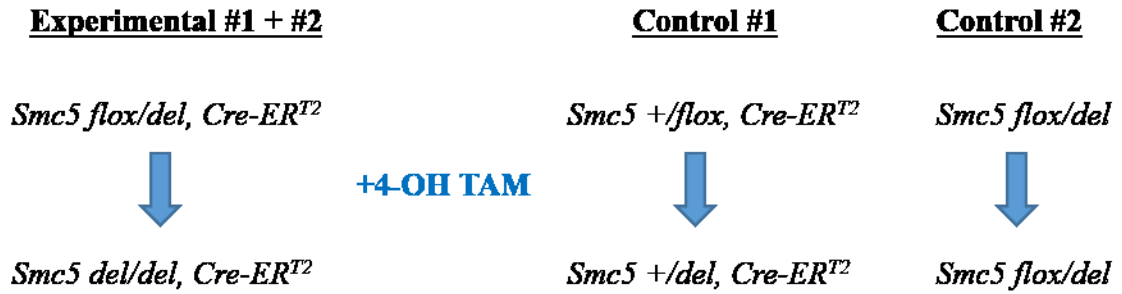
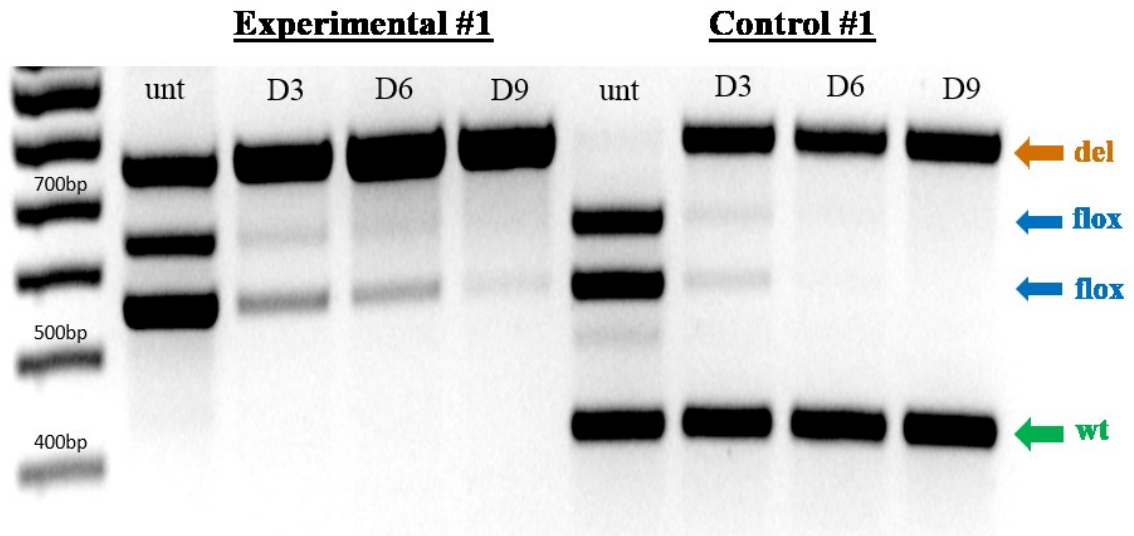


Figure 12 (A) Scheme of *Smc5* exon 4 deletion and primer positioning. Arrows (red) represent loxP sites. (B) Genotypes of cell lines used.

Confirmation of Smc5 knockout

A



B

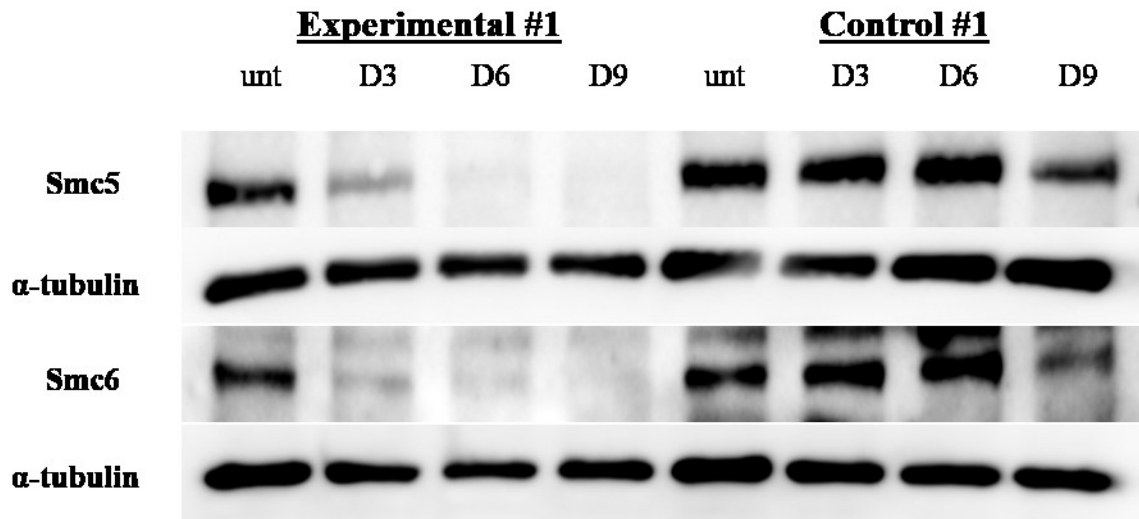


Figure 13 (A) PCR genotyping of experimental and control. (B) Western Blot confirming Smc5 and Smc6 depletion. Experimental and control cells were untreated (unt) or treated with 4-OH TAM for 3, 6, and 9 days (D3, D6, D9, respectively).

***Smc5* mutants exhibit decreased cell proliferation and aberrant mitosis**

Analogous to PCR and western blot data, *Smc5*-depleted cells demonstrated abnormal cell growth. 4-OH TAM-treated experimental cells showed a sustained ~1.5-2 fold decrease in cell growth by Day 6, while untreated experimental, untreated control, and 4-OH TAM-treated control cells demonstrated a consistent growth pattern (Figure 14). Despite slower proliferation, 4-OH TAM-treated experimental cells did not show evidence of cell death. All MEFs adhered to the cell culture vessel when plated, and did not display premature detachment.

Immunofluorescence microscopy analysis also showed several mitotic aberrancies after 6 days of 4-OH TAM treatment. We observed an increased formation of micronuclei, DNA bridges and lagging chromosomes in *Smc5*-depleted cells (Figure 15A-C). In comparison, untreated cells and 4-OH TAM-treated control cells showed significantly lower mitotic aberrancies. In addition, approximately 1 per 300 cells of the 4-OH TAM-treated experimental cells contained supernumerary chromosomes, providing evidence for inaccurate chromosome segregation (Figure 15 D).

Cell proliferation

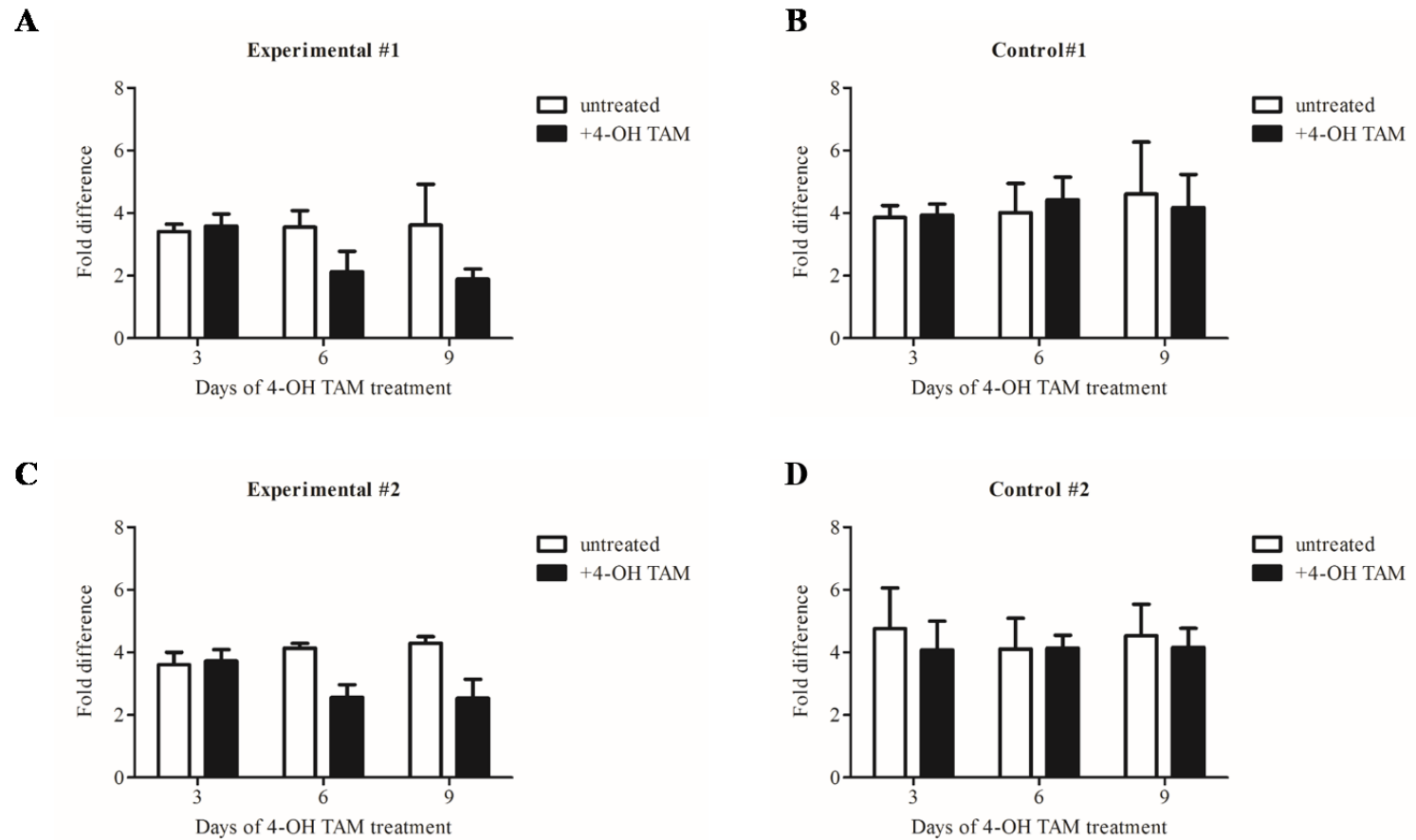


Figure 14 Cell proliferation of experimental and control MEFs. Cells were untreated (unt), or treated with 4-OH TAM for 3, 6, and 9 days (D3, D6, D9, respectively).

Mitotic aberrancies

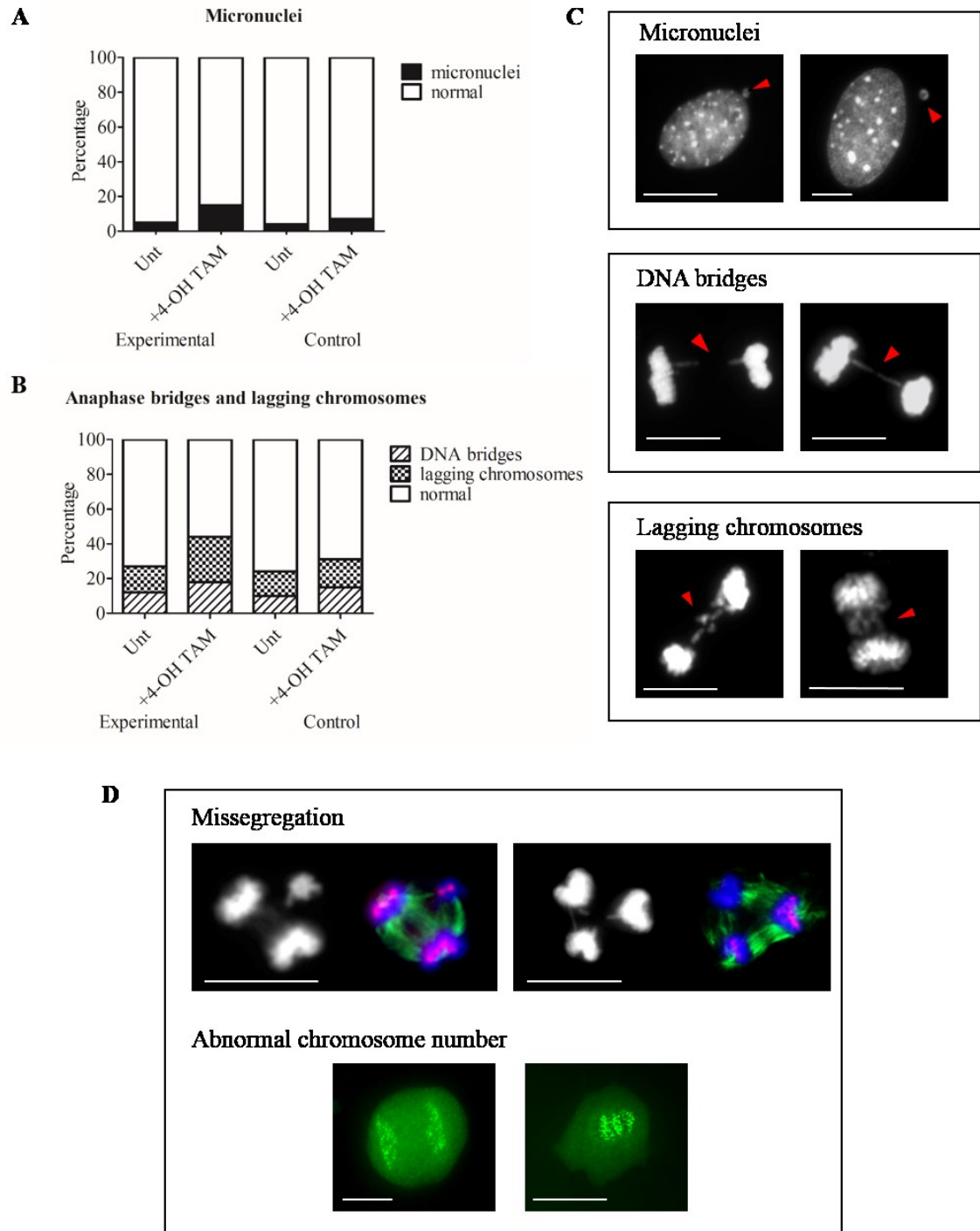


Figure 15 (A, B) Three hundred interphase and anaphase cells were analyzed per condition for micronuclei and bridges/lagging chromosomes, respectively. Bar graphs show mean from three independent experiments. (C) DAPI staining of cells with micronuclei, bridges, and lagging chromosomes, denoted by arrows. (D) Missegregation events and abnormal centromere numbers. Scale bar equals 10 μ m.

***Smc5* mutants demonstrate delayed entry into S-phase of cell cycle**

Based on observed cell growth characteristics, we hypothesized that *Smc5*-depleted cells would demonstrate abnormalities in cell cycle progression. To investigate this, we performed FACS analysis. Cells were synchronized in the G0/G1 phase via serum starvation and then released in serum-containing culture medium (see methods Figure 8). S-phase entry began at 15 hours post-serum release and reached a peak at 18 hours. Control #1 cells had 23% and 31% of cells in S-phase at 15 and 18 hours, respectively. After 4-OH TAM treatment, control #1 cells showed no appreciable differences (19% at 15 hours and 34% at 18 hours) (Figure 16 A, B). In control #2 cells, 19% and 37% of cells were in S-phase after 15 hours and 18 hours, respectively. In line with previous reports, 4-OH TAM treatment increased cell cycle progression in control #2 cells (Abukhdeir et al., 2007). Twenty-seven percent and 48% of cells were in S-phase after 15 and 18 hours, respectively (Figure 16 C, D).

In experimental MEFs, cell cycle progression was impeded after 4-OH TAM treatment. Similar to control cells, maximal number of cells were in S-phase 18 hours post-release. We did not observe a discernable difference in cell cycle progression between untreated and 4-OH TAM treated experimental #1 MEFs. At 18 hours, 27% and 25% of cells were in S-phase for untreated and 4-OH TAM treated cells, respectively (Figure 17 A,B). However, 4-OH TAM treated experimental #1 cells had a smaller proportion of cells at 18 hours in S-phase compared to 4-OH TAM treated control #1 cells (25% vs 34%, respectively). Experimental #2 cells demonstrated a delayed entry into S-phase. Untreated cells began entering S-phase at 15 hours post-serum release, while 4-OH TAM treated cells largely entered at 18 hours. At 15 hours, 26% of untreated

cells entered S-phase, while only 19% of 4-OH TAM treated cells were in S-phase.

Similarly, at 18 hours, 41% and 36% of untreated and 4-OH TAM treated cells were in S-phase, respectively (Figure 17 C, D). Despite differences in cell cycle dynamics, all cell lines still progressed to the G2 phase by 24 hours post-serum release.

Even though 4-OH TAM treatment increased cell cycle progression in control lines, 4-OH TAM treated experimental cells still had fewer cells in S-phase at the peak S-phase entry period of 18 hours. This suggests that the effect of 4-OH TAM was not enough to overcome Smc5 depletion. 4-OH TAM treated experimental #1 cells had 25% of cells in S-phase at 18 hours, while 4-OH TAM treated control #1 cells had 34% of cells in S-phase (Figure 18 A). Similarly, 4-OH TAM treated experimental #2 cells and 4-OH TAM treated control #2 cells had 33% and 48% of cells in S-phase at 18 hours, respectively (Figure 18 B). Although differences were not statistically significant ($p = 0.1751$), the trend we observe does suggest that Smc5 depletion is impacting cell cycle progression. Significant differences may arise upon treating cells with DNA damage agents, but may also affect cell viability.

FACS analysis: control cell lines

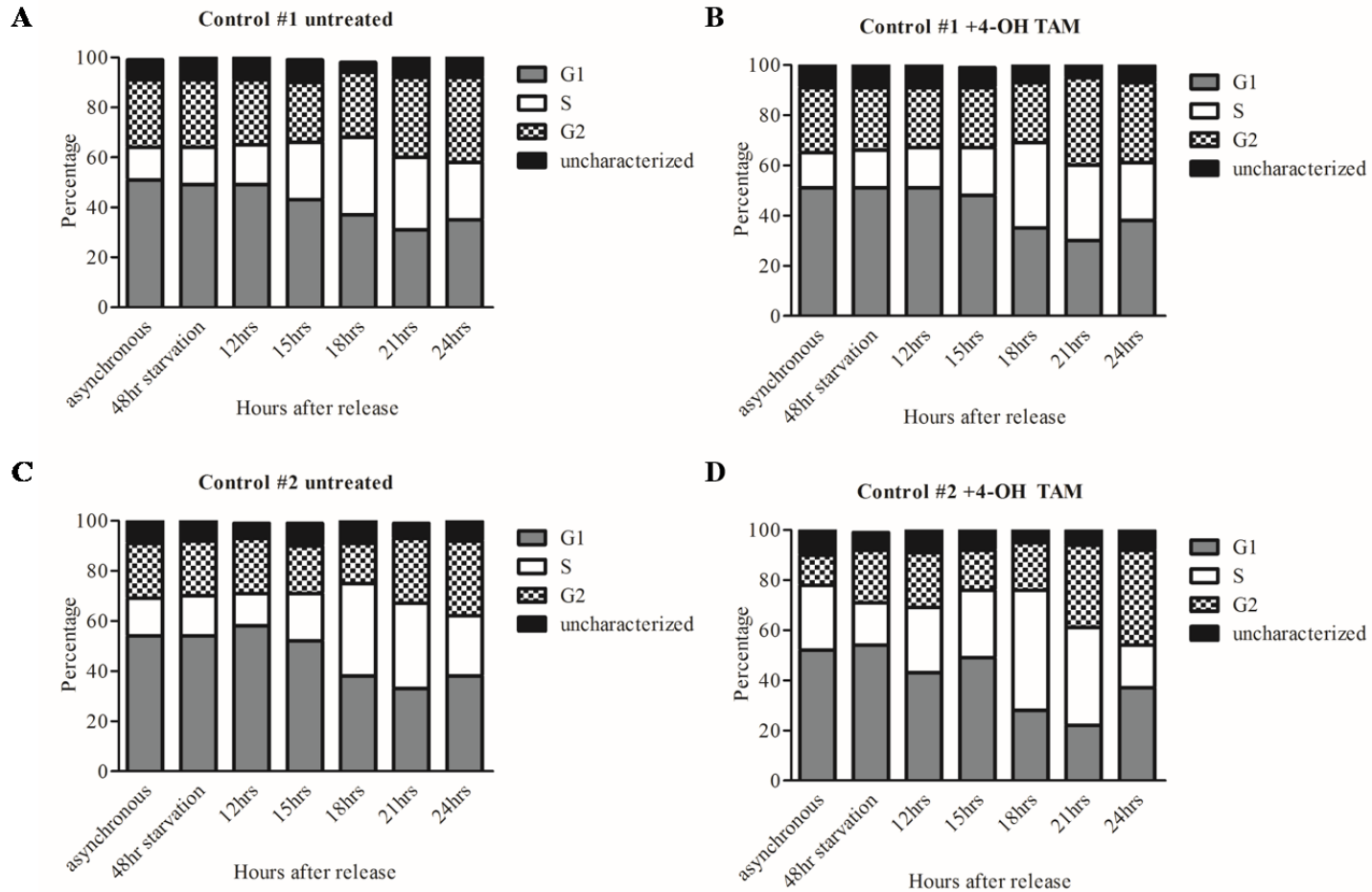


Figure 16 FACS analysis of control cells. Control #1 cells were (A) untreated or (B) 4-OH TAM-treated. Control #2 cells were also (C) untreated or (D) 4-OH TAM treated. Cells that were unable to be characterized are indicated as uncharacterized. Experiment was replicated three times and showed similar trends.

FACS analysis: experimental cell lines

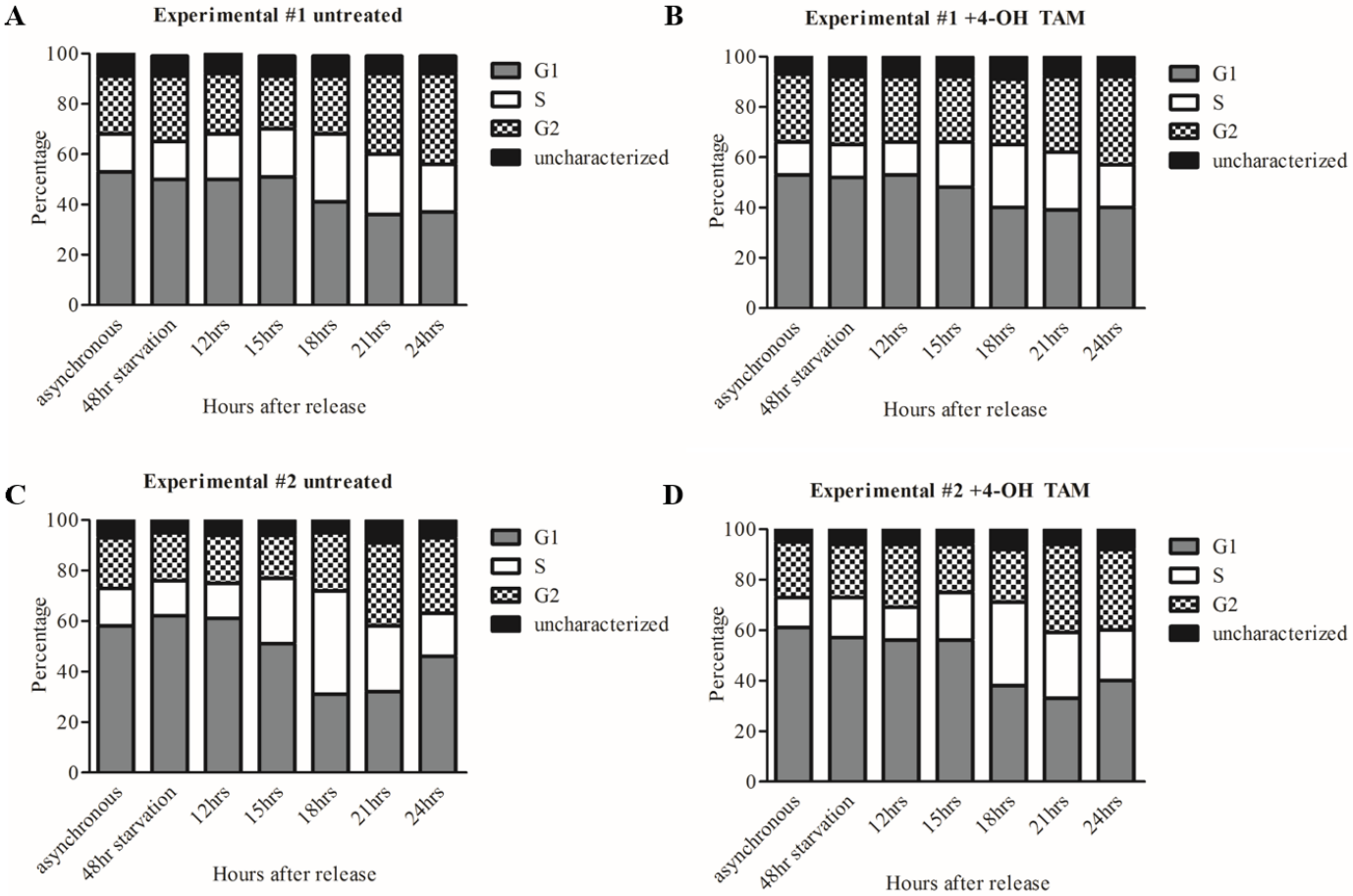
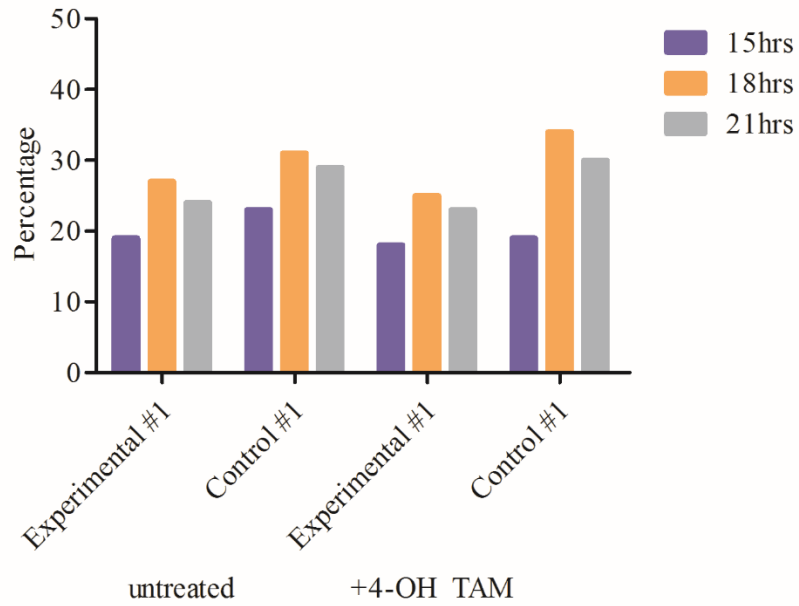


Figure 17 FACS analysis of experimental cells. Experimental #1 cells were (A) untreated or (B) 4-OH TAM-treated. Experimental #2 cells were also (C) untreated or (D) 4-OH TAM treated. Cells that were unable to be characterized are indicated as uncharacterized. Experiment was replicated three times and showed similar trends.

S-phase progression

A



B

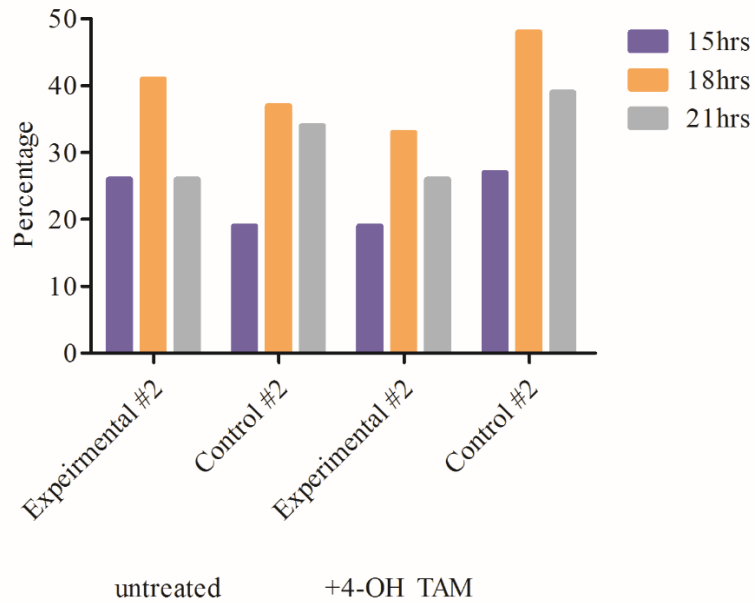


Figure 18 Percentage of cells in S-phase after 15, 18, and 21 hours of serum release in (A) experimental #1 and control #1 cells and (B) experimental #2 and control #2 cells before and after 4-OH TAM treatment.

Smc5 depletion leads to p53 accumulation

Decreased cell proliferation, chromosome segregation abnormalities and a delayed entry into S-phase suggest that Smc5 depleted cells were under mitotic stress. Based on these observations, we hypothesized that cells would be activating stress response pathways. We performed a western blot analysis to assess expression of the well-known stress response protein, p53. After 9 days of 4-OH TAM treatment, we found significant p53 accumulation in experimental cells, while control cells remained consistent (Figure 19). Experimental cells showed a 4.36 fold increase in p53 intensity before and after 9 days of 4-OH TAM treatment. In comparison, control cells only showed a fold difference of 0.85 before and after 4-OH TAM treatment.

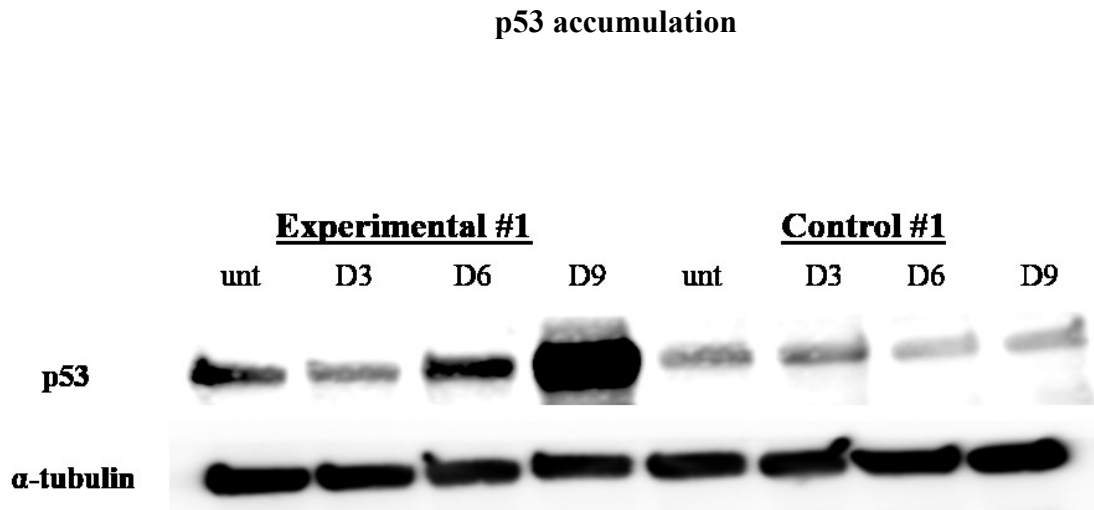


Figure 19 Western blot analysis of p53 expression in experimental and control MEF lines. Cells were either untreated (unt) or treated with 4-OH TAM for 3, 6, and 9 days (D3, D6, and D9, respectively). Experiment was replicated two times.

Smc5-depleted cells demonstrate heightened sensitivity to hydroxyurea and etoposide

Previous studies in yeast have reported heightened sensitivity to DNA damage agents in SMC protein deficient cells in yeast (reviewed in Stephan et al., 2011). Our observations of p53 accumulation suggest that Smc5-depleted cells are activating a DNA damage checkpoint response. Paired with our observations of delayed S-phase entry and mitotic aberrancies, we hypothesized that cells are not undergoing efficient DNA replication. We used two DNA damage agents, hydroxyurea and etoposide, to determine whether Smc5-depleted cells would be able to successfully activate DNA damage repair mechanisms and maintain viability. Hydroxyurea inhibits ribonucleotide reductase, depleting dNTPs and ultimately causing replication fork stalling (Osterman et al., 2013). Etoposide was used to induce double strand DNA breaks by stabilizing a cleavable complex via topoisomerase II inhibition (Maanen et al., 1988). Double strand DNA breaks are considered to be lethal lesions when not repaired.

Similar to yeast, Smc5-depleted cells showed an increase in DNA damage when treated with HU. 4-OH TAM treated experimental #1 cells showed an increase in mitotic abnormalities when compared to untreated experimental #1, untreated control #1 and 4-OH TAM treated control #1 cells (refer to Figure 8). Adding HU to cell culture for 24 hours exacerbated mitotic aberrancies primarily among 4-OH TAM-treated experimental #1 cells. DAPI staining revealed a 9% increase in micronuclei formation, 8% increase in DNA bridges, and 16% increase in lagging chromosomes after HU treatment (Figure 20).

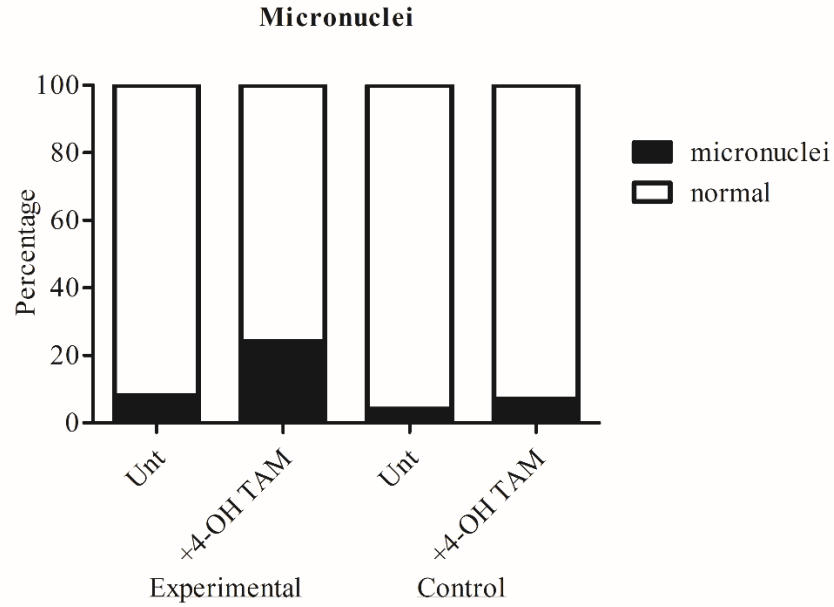
Treating Smc5-depleted cells with etoposide was much more devastating. After synchronizing cells, MEFs were cultured in normal medium with etoposide for 12 hours

and then allowed to recover in etoposide-free medium for another 12 hours. Treating Smc5 deficient cells with etoposide caused several mitotic catastrophes. These events included more severe versions of missegregation events, micronuclei accumulation, DNA bridge formation, and lagging chromosomes. Twenty-four percent 4-OH TAM-treated experimental #1 cells showed one or more types of mitotic abnormalities. In comparison, only 8-14% of untreated experimental #1, untreated control #1 and 4-OH TAM-treated control #1 cells demonstrated mitotic aberrancies.

Additionally, adding etoposide to cell culture caused cells to undergo nuclear fragmentation. Twenty-two to thirty percent of untreated experimental #1, untreated control #1, and 4-OH-TAM treated control #1 cells demonstrated nuclear fragmentation. In 4-OH TAM treated experimental #1 cells, almost 50% of 4-OH TAM treated cells were fragmented, suggesting insurmountable stress in Smc5-depleted cells (Figure 21).

Defects observed in hydroxyurea-treated MEFs

A



B

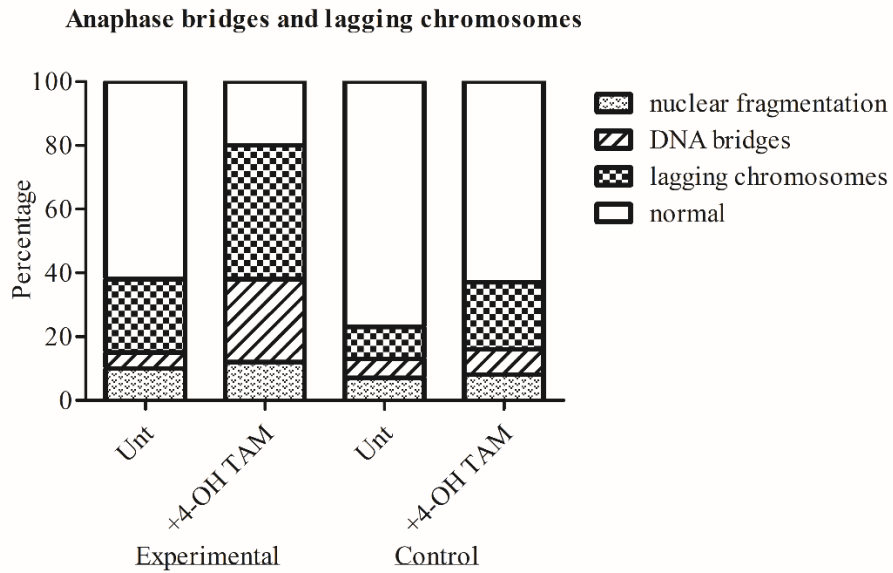
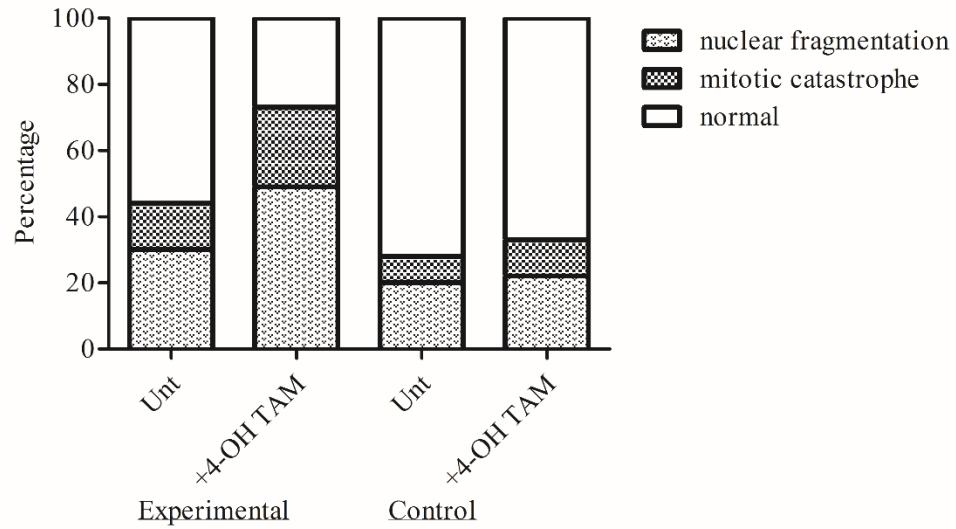


Figure 20 (A) Micronuclei formation and (B) anaphase bridges and lagging chromosome accumulation after hydroxyurea treatment. Three-hundred interphase and anaphase cells were analyzed in three independent experiments. Bar graphs represent mean.

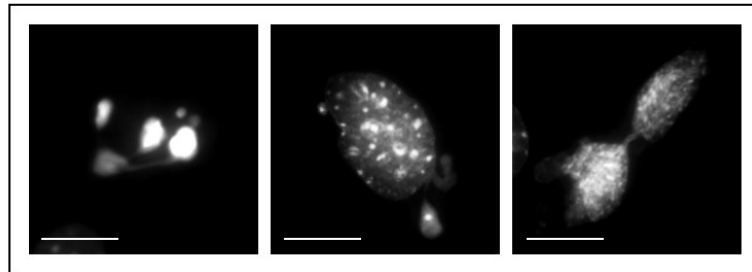
Defects observed in etoposide-treated MEFs

A



B

Mitotic catastrophes



C

Nuclear fragmentation

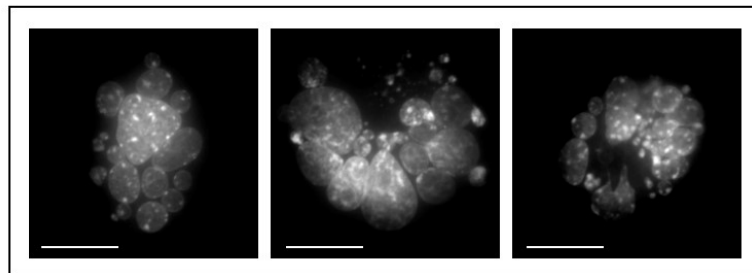


Figure 21 (A) Nuclear fragmentation and mitotic catastrophes were quantified in etoposide treated MEFs. Three-hundred cells were evaluated in three independent collections. Bar graphs represent mean. (B) DAPI stained cells with examples of mitotic catastrophes and (C) nuclear fragmentation. Scale bar equals 10 μ m.

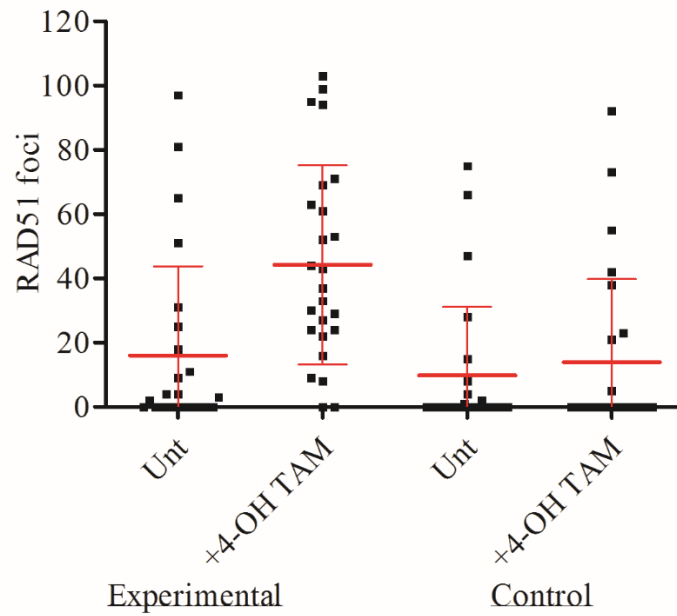
Hydroxyurea treatment leads to increased Rad51 accumulation in *Smc5*-depleted MEFs

In order to further characterize replication-related DNA repair pathways, we used immunostaining to investigate Rad51 accumulation. Replication fork stalling agents, such as hydroxyurea, induce activation of DNA damage repair pathways such as homologous recombination (HR) in order to promote cell survival. If replication forks are kept stalled, double strand DNA breaks may occur. Rad51 has been identified as key player in both HR and non-HR pathways (Peterman et al., 2010). For HR pathways, Rad51 mediates re-start of replication forks by promoting single strand DNA stabilization and strand invasion. Additionally, it has been reported from studies using budding yeast and *Drosophila melanogaster* cell culture that *Smc5/6* excludes Rad51 foci to prevent incorrect strand invasion and abnormal recombination specifically within heterochromatin enriched for repetitive DNA sequences (Eckert-Boulet et al., 2009; Chiolo et al., 2011).

Because *Smc5* mutants exhibited hypersensitivity to hydroxyurea treatment, we hypothesized that cells would be unable to undergo faithful HR and accumulate Rad51 foci. MEFs were treated with hydroxyurea and allowed to recover in normal medium for 25 hours. Despite the allowed recovery time, *Smc5* mutants had ~44% increase in cells containing Rad51 foci compared to controls. *Smc5*-depleted cells averaged 40 foci per cell, while control cells averaged 14 foci per cell ($p=0.0019$) (Figure 22).

Rad51 accumulation in hydroxyurea-treated MEFs

A



B

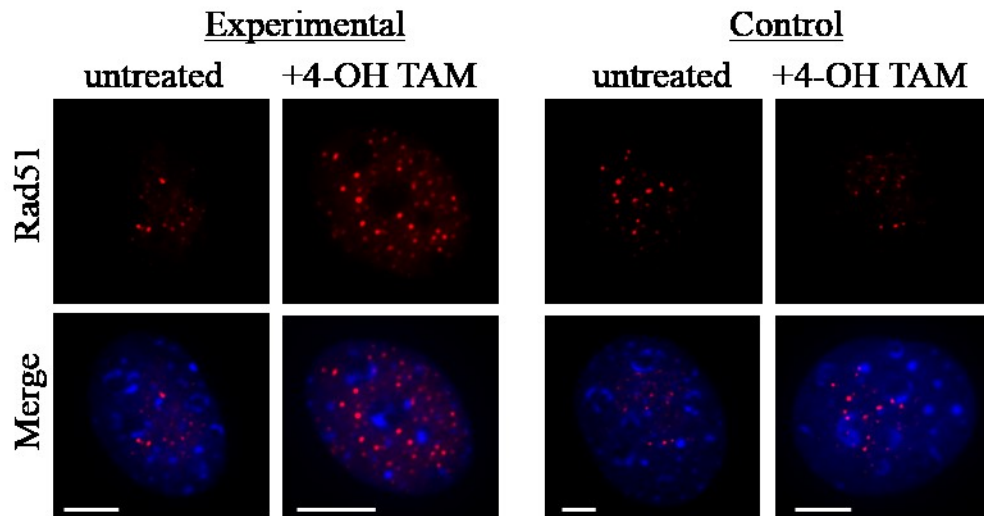


Figure 22 (A) Rad51 foci in hydroxyurea-treated MEFs (n=25). (B) Samples of Rad51 accumulation in hydroxyurea treated MEFs. Scale bar equals 10 μ m.

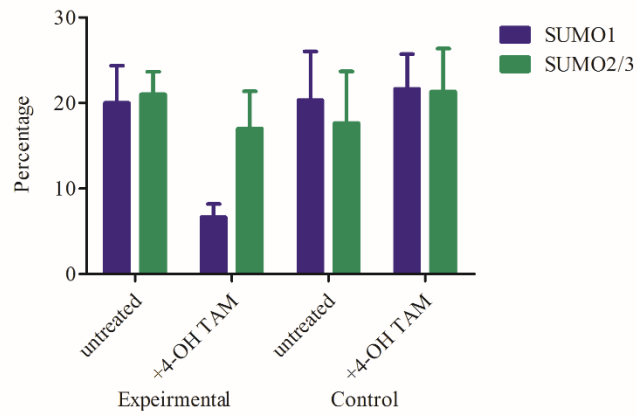
Smc5/6 depletion leads to a decrease in SUMO1 but not SUMO2/3 foci in hydroxyurea-treated cells

Sumoylation has been cited as an important mechanism for DNA damage response and repair (Potts, 2009). In yeast, Nse2 mutations have been shown to cause a Rad51-dependent accumulation of X-shaped DNA structures (Branzei et al., 2006). It also been reported that SUMO noncovalently interacts with Rad51 at damaged replication forks to modulate HR (Ouyang et al., 2009). Based on this, we hypothesized that hydroxyurea-treated MEFs would show SUMO accumulation.

We investigated both SUMO1 and SUMO2/3, and found differential expression. In hydroxyurea-treated MEFs, about 15-20% of untreated control cells, 4-OH TAM treated control cells and untreated experimental cells contained SUMO1 and SUMO2/3 foci. 4-OH-TAM treated experimental cells showed a comparable number of SUMO2/3 accumulation, but not SUMO1. Seven percent of Smc5 depleted MEFs exhibited SUMO1 foci, suggesting that Smc5/6 is affecting the SUMO1 regulatory pathway (Figure 23).

SUMO1 and SUMO2/3 accumulation in hydroxyurea treated MEFs

A



B

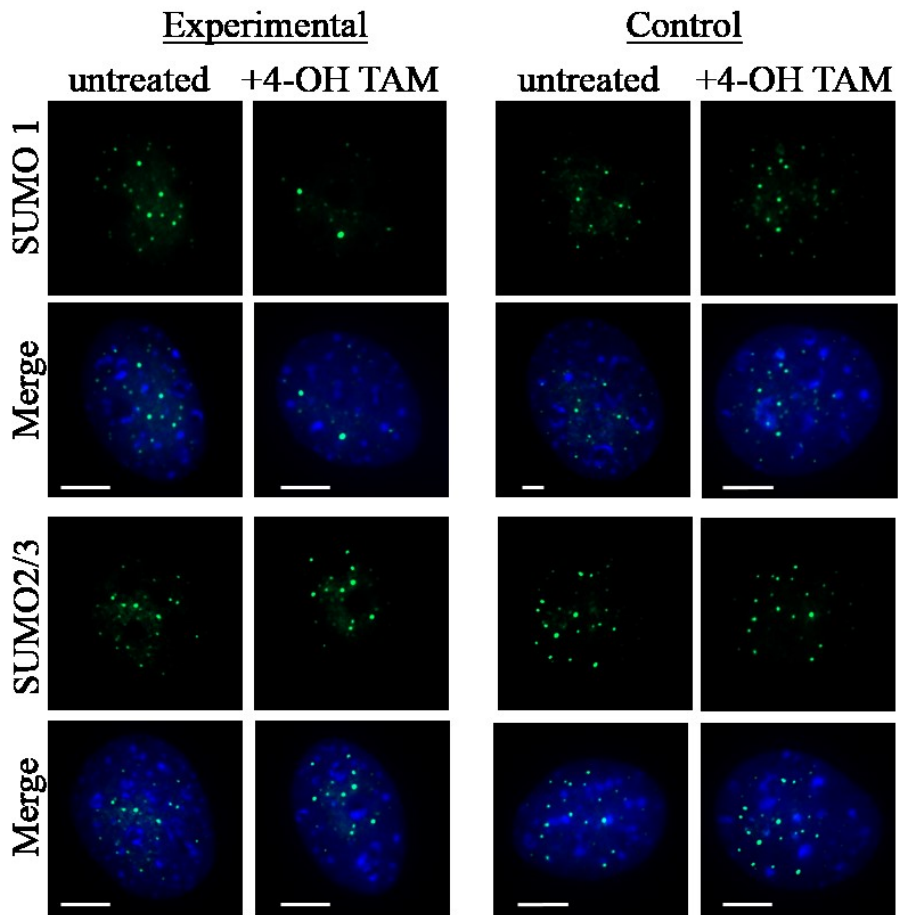


Figure 23 (A) Cells containing SUMO1 and SUMO2/3. Three-hundred cells were assessed in 3 independent collections. (B) Samples of SUMO accumulation in MEFs. Scale bar equals 10 μ m.

Discussion

So far, the role of Smc5/6 has largely been studied in lower organisms. Only a few studies have used mouse and human models to elucidate the functionality of Smc5/6. In the handful of studies that did use mouse and human cells, siRNA was used to knockdown Smc5 and Smc6. This method, however, was found to cause off target effects. Therefore, previous findings suggesting that the Smc5/6 complex is required for maintenance of sister chromatid cohesion, together with suggestions that the Smc5 and Smc6 have independent functions are false (Wu et al., 2012). In this study, we used immortalized MEFs so that we could consistently manipulate cells and gain reproducible results. Though our model used a conditional knockout of *Smc5*, we observed a complimentary decline in Smc6 protein levels, suggesting that the entire Smc5/6 complex was destabilized.

Unlike in fission and budding yeast cells, Smc5/6 is not essential for MEF viability. However, Smc5-depleted MEFs demonstrated a 1.5-2 fold decrease in proliferation compared to control cells. A similar trend was observed in a Smc5/6 knockdown model in RPE-1 cells. At 5 days post-transfection with Smc5 siRNA, the cell number dropped by about half. Control cells proliferated to 15 million, while Smc5-depleted cells only grew to only 8 million (Gallego-Paez et al., 2014). In chicken cells, a more drastic drop was observed. After 3 days, there were a total of 8 million wild type cells, and only 2 million Smc5 depleted cells (Stephan et al., 2011).

Decreased cell proliferation has been associated with compromised mitotic processes and replication stress (Gelot et al., 2015). We used immunofluorescence microscopy to visualize mitotic aberrancies. DAPI staining revealed an increase in DNA bridge formation, micronuclei accumulation, lagging chromosomes and missegregation

events in *Smc5*-depleted MEFs. These phenotypes have been consistently observed in other RNAi-mediated *Smc5/6* knockdowns. In human RPE-1 *Smc5* deficient cells, ~30% of cells accumulated anaphase bridges and lagging chromosomes (vs. 10% in controls). In MEFs we observed closer to 50% (vs. ~30% in controls) (Gallego-Paez et al., 2012). Compared to baseline levels, our cells demonstrated comparable results. Human *NSE2* mutants, however, had substantially lower micronuclei formation compared to our mutants MEFs. *NSE2* mutants demonstrated ~6% micronuclei formation (Payne et al., 2014), while our MEF *Smc5* mutants showed almost 20%. Our MEFs may have shown higher micronuclei formation due to the entire complex being compromised, versus only a *NSE2* mutation in human cells. Similar to our knockout MEFs, missegregation events, and lagging chromosomes were also observed in *Smc5* depleted chicken cells (Stephan et al., 2011).

Based on these observations, we next evaluated cell cycle progression. Similar to *Smc6* mutants in budding yeast (Torres et al., 2007), our FACS analysis revealed that *Smc5* depleted cells showed a delayed entry into S-phase, but still progressed to G2 phase. In contrast, flow cytometry in chicken cells showed no difference in cell cycle distribution. *Smc5* mutants and control cells had an equal amount of cells in G1, S, and G2-phase. However, *Smc5*-depleted chicken cells had a higher mitotic index than wild type cells. The ratio of cells entering mitosis vs. not entering mitosis was higher in *Smc5*-depleted cells, suggesting impaired mitotic regulation. (Stephan et al., 2011). Other studies have shown that *Smc5/6* mutants enter the cells cycle without completing DNA damage repair, leading to aberrant mitosis (Verkade et al., 1999; Harvey et al., 2004; Andrews et al., 2005; Ampatzidou et al., 2006; Miyabe et al., 2006). Because we did not

observe accumulation of MEFs in G2 phase, Smc5-deficient cells could be entering mitosis without repairing DNA damage. This further supports our observation of DNA bridges and lagging chromosomes.

We also observed an upregulation of p53. p53 regulates several aspects of cell cycle processes. It inhibits re-replication after DNA damage by blocking S-phase entry. The p53 accumulation we observe parallels the delay in S-phase entry demonstrated in our FACS analysis. Additionally, p53 is important for the G2/M transition, and was shown to inhibit mitotic entry when DNA synthesis is blocked (Taylor et al., 1999). This could explain the overall slower cell growth observed in Smc5 mutants. To our knowledge, p53 has not been assessed in Smc5/6-deficient cells.

Previous studies have shown Smc5/6 mutants to be hypersensitive to DNA damage agents both in lower organisms and mammalian models (reviewed in Stephan et al., 2011). Similarly, our Smc5 mutant cells showed heightened sensitivity to hydroxyurea and etoposide treatment. Both treatments lead to an increase in mitotic abnormalities (micronuclei, DNA bridges, lagging chromosomes, and missegregation) compared to controls. Additionally, ~50% of etoposide-treated cells underwent nuclear fragmentation, whereas only 20-30% of control cells displayed this phenomenon. This suggests that etoposide-induced DSBs may be creating insurmountable stress in Smc5-depleted MEFs, further supporting Smc5's crucial role in DNA damage repair.

Based on observed hypersensitivity to DNA damage, we investigated DNA damage repair mechanisms. In yeast, Smc5/6 has been heavily implicated with HR-mediated DNA damage repair during S-phase (reviewed in Wu and Ku et al., 2012). Rad51 is associated with HR and mediates strand invasion at stalled replication forks (Li

et al., 2008). In order to observe mitotic progression and recovery after replication fork stalling, we treated cells with hydroxyurea for 24 hours, and then synchronized them in HU-free medium for an additional 24 hours. Despite having 24 hours to recover, Smc5-deficient MEFs showed an accumulation of Rad51 puncta. Our observation supports that Smc5 plays a role in HR-dependent repair pathways.

In *Drosophila melanogaster*, it was suggested that Smc5/6 promotes expansion and relocalization of the damaged DNA segment to heterochromatin periphery in order to prevent abnormal Rad51-mediated recombination. Smc5/6 components localized to the HP1a domain during interphase and disassembled during mitosis (Chiolo et al., 2011). Similarly in *S. pombe*, Smc5/6 was shown to be recruited to pericentromeric heterochromatin after HU treatment, presumably for the repair of stalled replication forks (Pebernard et al., 2008). In our study, Rad51 puncta were not localized to heterochromatin. Therefore, we hypothesize that damaged DNA segments may be able to expand and relocalize outside of the heterochromatin domain for repair, but ultimately the recombination event cannot be resolved in the absence of the Smc5/6 complex.

Because we did not observe any nuclear fragmentation or cell death in HU-treated cells, we propose that MEFs are using other DNA damage repair mechanisms, such as NHEJ, to preserve cell viability. In yeast, it was shown that Smc5/6 plays an exclusive role in HR repair, and is not needed for NHEJ (De Piccoli, Cortes-Ledesma et al., 2006). Additionally, SUMOylation has been identified as an important post-translational modification in DNA damage repair mechanisms (Wu and Kong et al., 2012). SUMO1 has been associated with HR and non-HR repair pathways, while SUMO2/3 is primarily associated with non-HR pathways (Hu et al., 2014). Our observation of SUMO1 decline

in *Smc5* mutants, but not SUMO2/3, suggests that Smc5/6 regulates or associates with SUMO function. This further supports that MEF *Smc5* mutants are primarily deficient in HR-repair capabilities, similar to yeast mutants.

For the first time, we have validated the importance of Smc5 in mouse cells. Our data is consistent with many of the phenotypes observed in yeast, *Drosophila*, chicken, and human models. We are the first to show evidence of significant p53 upregulation, and differences in SUMO1 vs. SUMO2/3 modification. In addition, we have developed a model cell line that allows targeted mutation of a Smc5/6 component, which is not subject to off-target effects seen in previous work using siRNA knockdown. Future work should delineate other aspects of the p53 regulatory pathway to further characterize how Smc5 is impacting cellular stress response. Similarly, SUMO1 and SUMO2/3 modification should be further studied to identify underlying SUMOylation pathways.

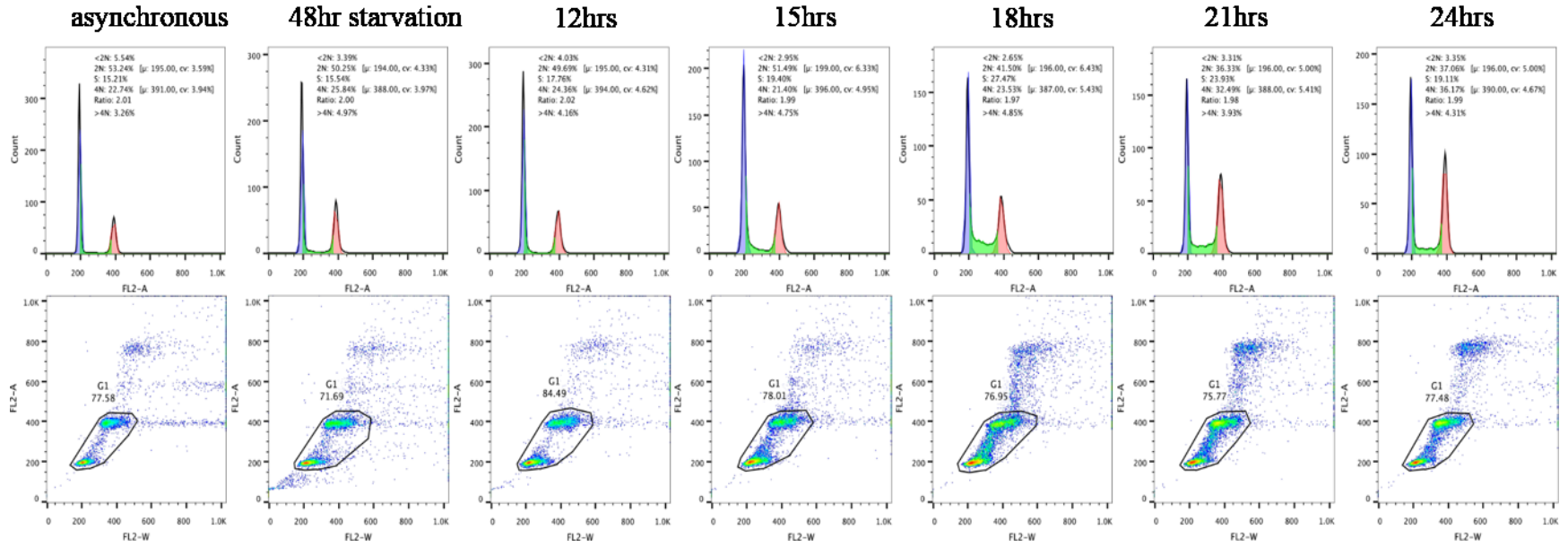
Public Health Relevance

Due to the widespread role of SMC complexes in the cell cycle, mutations in SMC proteins have been associated with rare, but severe developmental disorders. Two such disorders, Cornelia de Lange syndrome and Roberts's syndrome, are associated with craniofacial abnormalities, mental retardation, limb defects, and gastrointestinal problems. Onset of symptoms can occur pre or post-natal, and are usually recognized early on from delayed growth patterns. Sixty-five percent of individuals affected with Cornelia de Lange syndrome show mutations in cohesin subunits *Smc1*, *Smc3*, and in the cohesin regulatory protein, *NIPBL*. Almost all cases have been identified as dominant and sporadic (Liu et al., 2010). In contrast, Roberts's syndrome is inherited as an autosomal recessive trait. However, defects in Robert's syndrome patients are also attributed to cohesin pathways. The establishment of cohesin 1 homolog 2 (*ESCO2*) protein was found to be disrupted, causing premature chromosome segregation primarily on chromosomes 1, 9, and 16 (Vega et al., 2010).

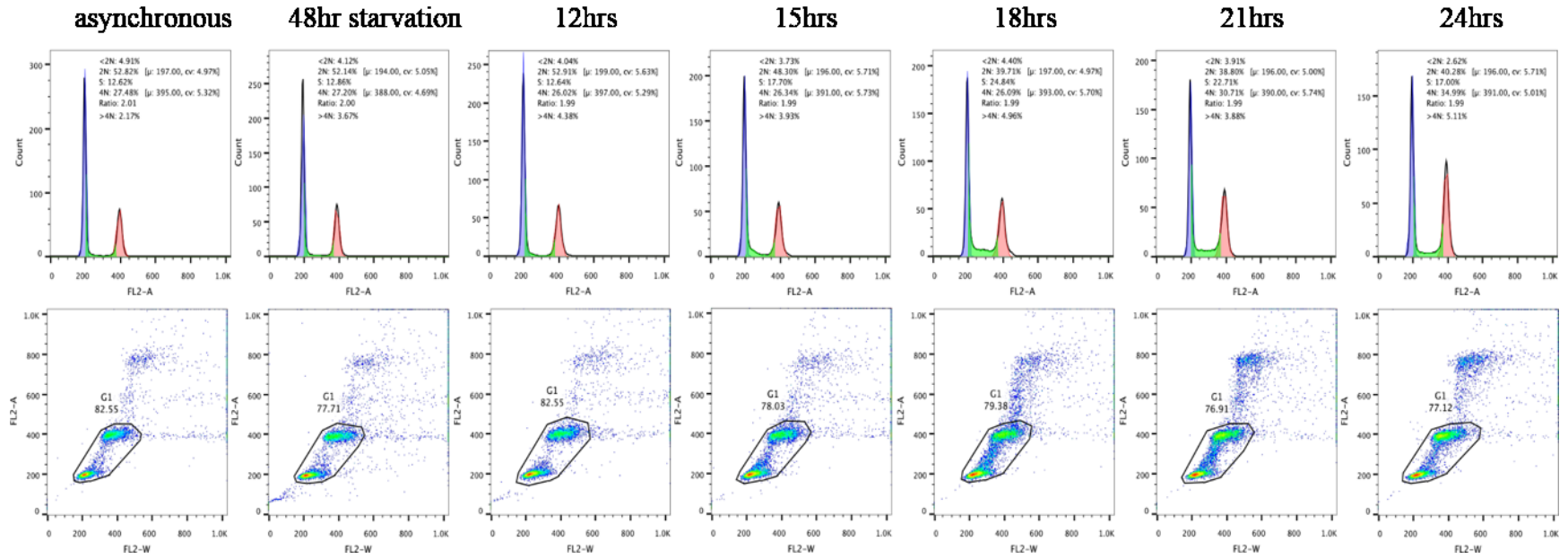
Disorders caused by *Smc5/6* mutations are less well characterized. However, similar devastating phenotypes have been observed in patients. Mutations in *NSE2* have been associated with primordial dwarfism and microcephaly (Payne et al, 2014). Additionally, about 10% of sequenced cancers have been associated with mutations in the *Smc5/6* subunits (Stevens et al, 2011). One hypothesis is that *Smc5/6* mutation-induced stalled replication forks cause a pathological accumulation of X-shaped DNA structures, ultimately compromising genomic integrity, cell cycle progression and thus development (Branzei et al., 2006).

Today, SMC-associated disorders have no cure. Furthermore, there still remains a large gap between SMC cell biology and the etiology of human diseases. SMC research efforts are important for closing this gap, and shaping the field of medical genetics.

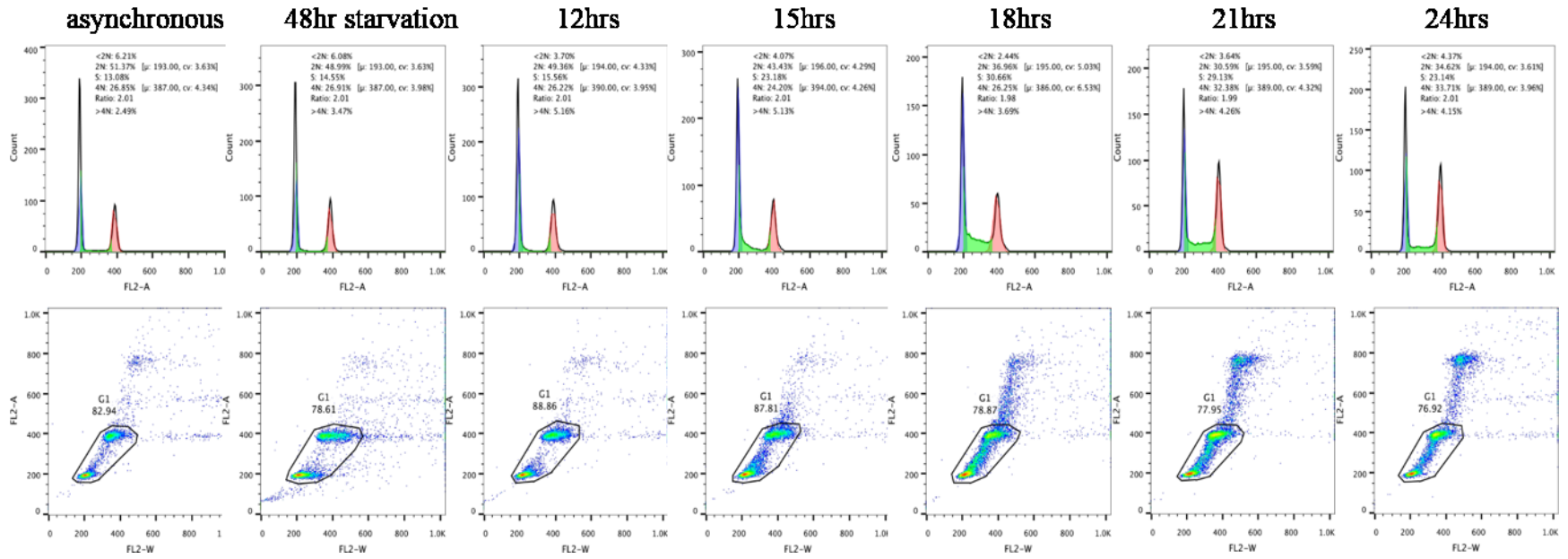
Supplemental Figure 1: FACS analysis of Experimental #1 untreated



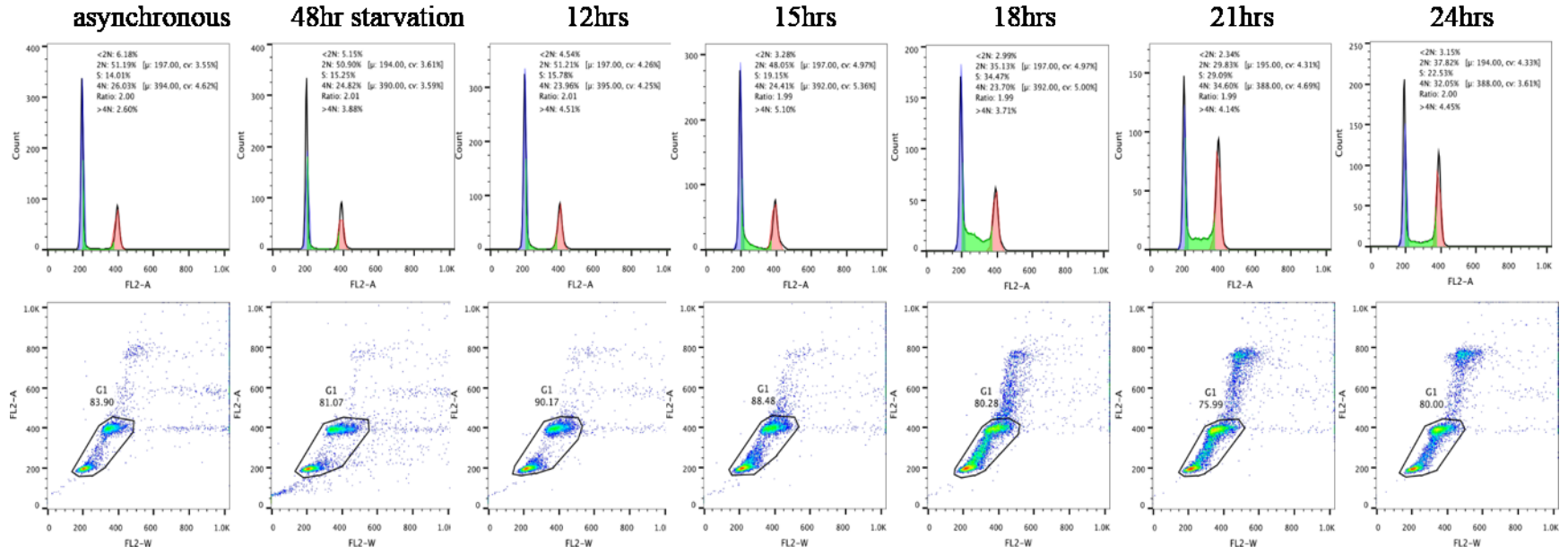
Supplemental Figure 2: FACS analysis of Experimental #1 +4-OH TAM



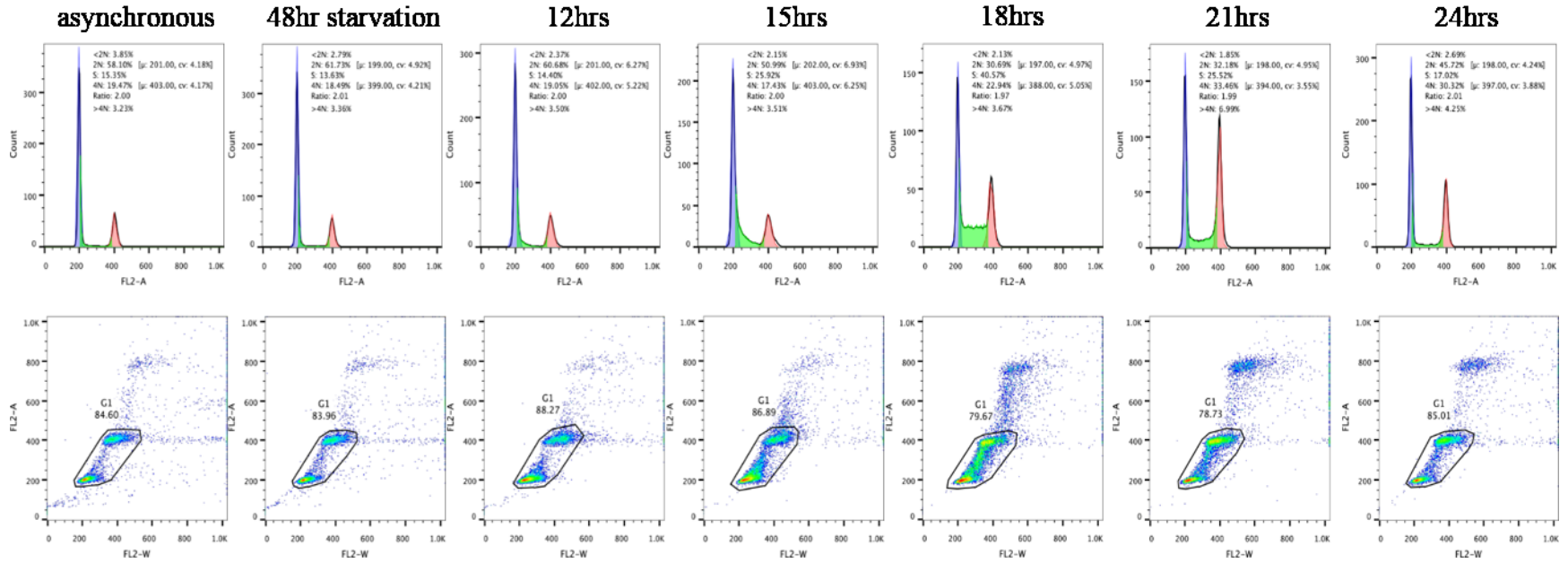
Supplemental Figure 3: FACS analysis of Control #1 untreated



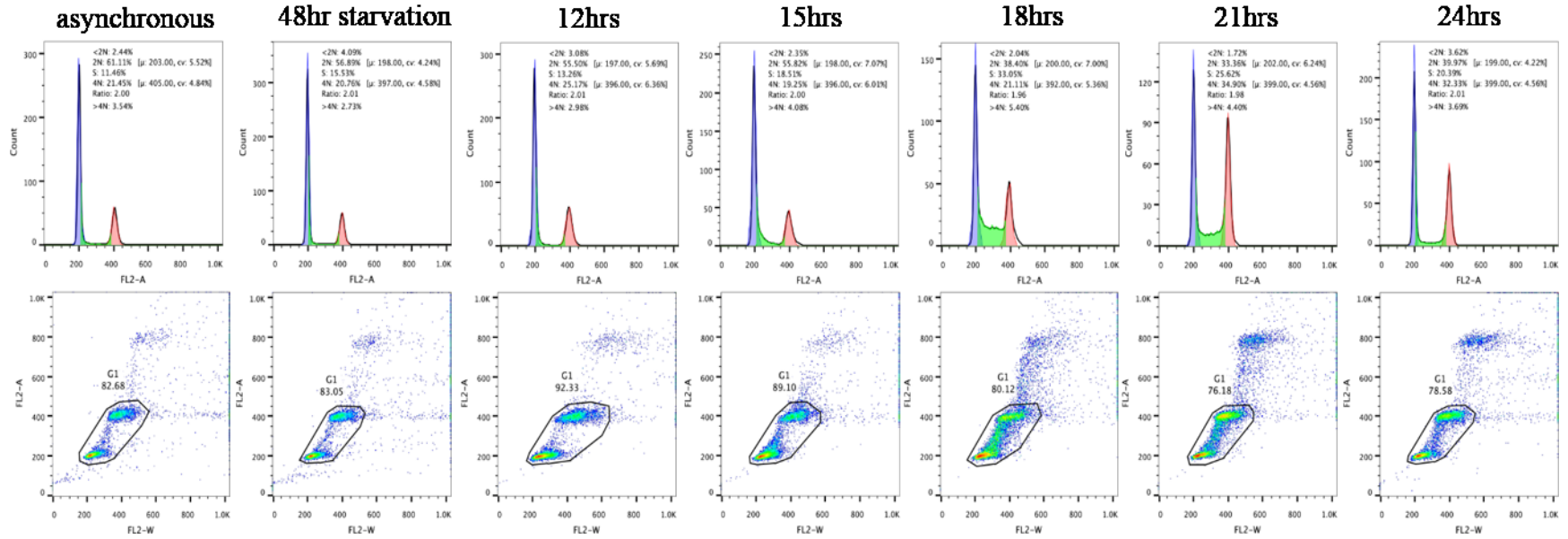
Supplemental Figure 4: FACS analysis of Control #1 +4-OH TAM



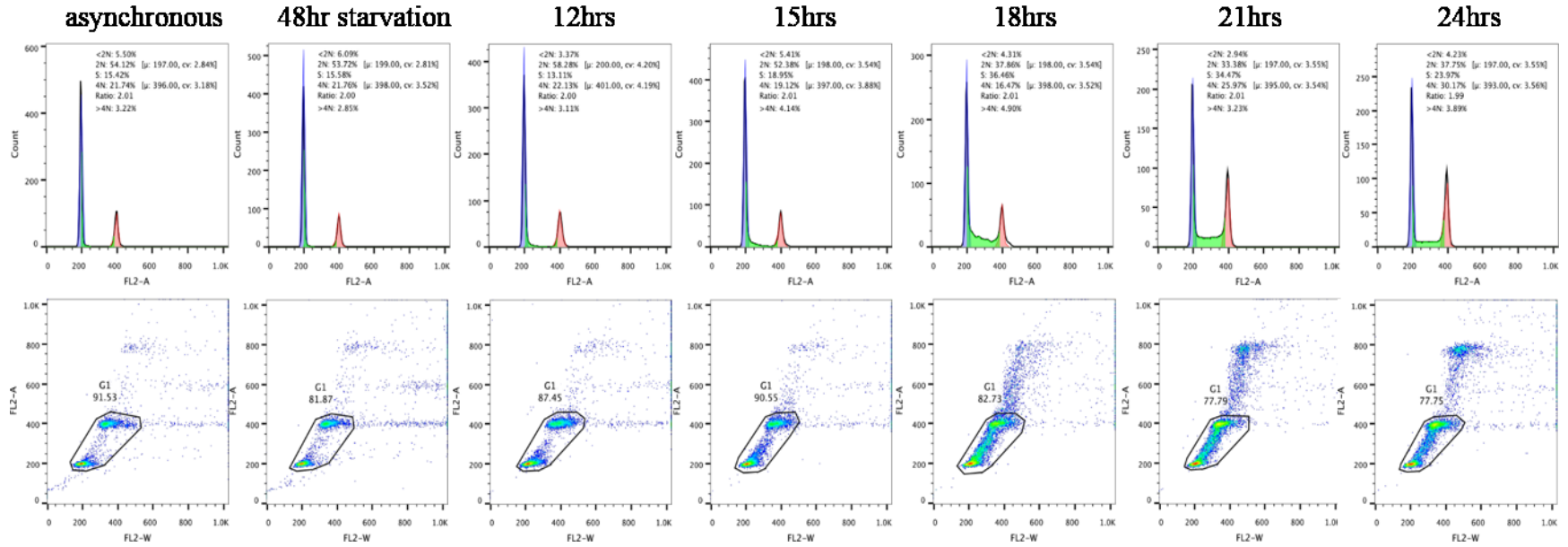
Supplemental Figure 1: FACS analysis of Experimental #2 untreated



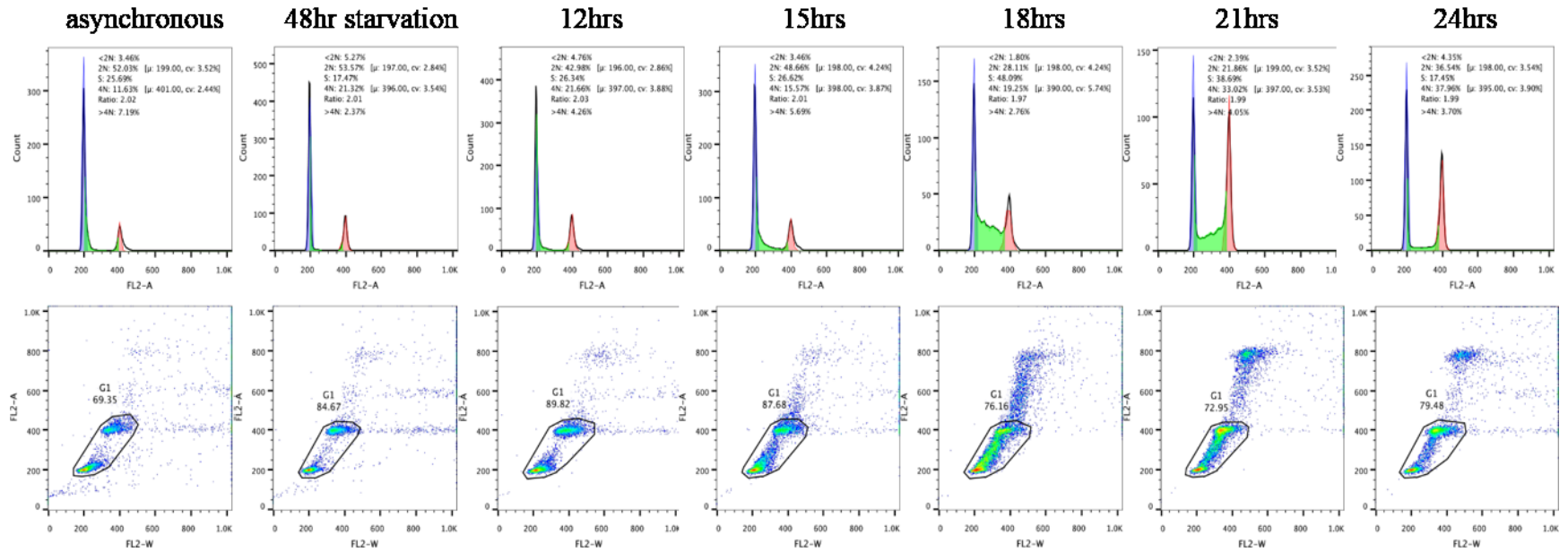
Supplemental Figure 6: FACS analysis of Experimental #2 +4-OH TAM



Supplemental Figure 7: FACS analysis of Control #2 untreated



Supplemental Figure 8: FACS analysis of Control #2 +4-OH TAM



References

- Ampatzidou, E., Irmisch, A., O'Connell, M. J., & Murray, J. M. (2006). Smc5/6 is required for repair at collapsed replication forks. *Mol Cell Biol*, 26(24), 9387-9401. doi: 10.1128/mcb.01335-06
- Andrews, E. A., Palecek, J., Sergeant, J., Taylor, E., Lehmann, A. R., & Watts, F. Z. (2005). Nse2, a component of the Smc5-6 complex, is a SUMO ligase required for the response to DNA damage. *Mol Cell Biol*, 25(1), 185-196. doi: 10.1128/mcb.25.1.185-196.2005
- Beasley, M., Xu, H., Warren, W., & McKay, M. (2002). Conserved disruptions in the predicted coiled-coil domains of eukaryotic SMC complexes: implications for structure and function. *Genome Res*, 12(8), 1201-1209. doi: 10.1101/gr107302
- Behlke-Steinert, Susanne, Touat-Todeschini, Leila, Skoufias, Dimitrios A., & Margolis, Robert L. (2014). SMC5 and MMS21 are required for chromosome cohesion and mitotic progression. *Cell Cycle*, 8(14), 2211-2218. doi: 10.4161/cc.8.14.8979
- Bermudez-Lopez, M., Ceschia, A., de Piccoli, G., Colomina, N., Pasero, P., Aragon, L., & Torres-Rosell, J. (2010). The Smc5/6 complex is required for dissolution of DNA-mediated sister chromatid linkages. *Nucleic Acids Res*, 38(19), 6502-6512. doi: 10.1093/nar/gkq546
- Branzei, D., Sollier, J., Liberi, G., Zhao, X., Maeda, D., Seki, M., . . . Foiani, M. (2006). Ubc9- and mms21-mediated sumoylation counteracts recombinogenic events at damaged replication forks. *Cell*, 127(3), 509-522. doi: 10.1016/j.cell.2006.08.050
- Carlborg, K. K., Kanno, T., Carter, S. D., & Sjogren, C. (2015). Mec1-dependent phosphorylation of Mms21 modulates its SUMO ligase activity. *DNA Repair (Amst)*, 28, 83-92. doi: 10.1016/j.dnarep.2015.01.006
- Chen, Y. H., Szakal, B., Castellucci, F., Branzei, D., & Zhao, X. (2013). DNA damage checkpoint and recombinational repair differentially affect the replication stress tolerance of Smc6 mutants. *Mol Biol Cell*, 24(15), 2431-2441. doi: 10.1091/mbc.E12-11-0836
- Chiolo, I., Minoda, A., Colmenares, S. U., Polyzos, A., Costes, S. V., & Karpen, G. H. (2011). Double-strand breaks in heterochromatin move outside of a dynamic HP1a domain to complete recombinational repair. *Cell*, 144(5), 732-744. doi: 10.1016/j.cell.2011.02.012
- Copsey, A., Tang, S., Jordan, P. W., Blitzblau, H. G., Newcombe, S., Chan, A. C., . . . Hoffmann, E. (2013). Smc5/6 coordinates formation and resolution of joint molecules with chromosome morphology to ensure meiotic divisions. *PLoS Genet*, 9(12), e1004071. doi: 10.1371/journal.pgen.1004071
- David, G., Turner, G. M., Yao, Y., Protopopov, A., & DePinho, R. A. (2003). mSin3-associated protein, mSds3, is essential for pericentric heterochromatin formation and chromosome segregation in mammalian cells. *Genes Dev*, 17(19), 2396-2405. doi: 10.1101/gad.1109403
- De Piccoli, G., Cortes-Ledesma, F., Ira, G., Torres-Rosell, J., Uhle, S., Farmer, S., . . . Aragon, L. (2006). Smc5-Smc6 mediate DNA double-strand-break repair by promoting sister-chromatid recombination. *Nat Cell Biol*, 8(9), 1032-1034. doi: 10.1038/ncb1466
- De Piccoli, G., Torres-Rosell, J., & Aragon, L. (2009). The unnamed complex: what do we know about Smc5-Smc6? *Chromosome Res*, 17(2), 251-263. doi: 10.1007/s10577-008-9016-8
- Doerks, T., Copley, R. R., Schultz, J., Ponting, C. P., & Bork, P. (2002). Systematic identification of novel protein domain families associated with nuclear functions. *Genome Res*, 12(1), 47-56. doi: 10.1101/
- Eckert-Boulet, N., & Lisby, M. (2009). Regulation of rDNA stability by sumoylation. *DNA Repair (Amst)*, 8(4), 507-516. doi: 10.1016/j.dnarep.2009.01.015
- Gallego-Paez, L. M., Tanaka, H., Bando, M., Takahashi, M., Nozaki, N., Nakato, R., . . . Hirota, T. (2014). Smc5/6-mediated regulation of replication progression contributes to chromosome assembly during mitosis in human cells. *Mol Biol Cell*, 25(2), 302-317. doi: 10.1091/mbc.E13-01-0020
- Gelot, C., Magdalou, I., & Lopez, B. S. (2015). Replication stress in Mammalian cells and its consequences for mitosis. *Genes (Basel)*, 6(2), 267-298. doi: 10.3390/genes6020267
- Gomez, R., Jordan, P. W., Viera, A., Alsheimer, M., Fukuda, T., Jessberger, R., . . . Suja, J. A. (2013). Dynamic localization of SMC5/6 complex proteins during mammalian meiosis and mitosis suggests functions in distinct chromosome processes. *J Cell Sci*, 126(Pt 18), 4239-4252. doi: 10.1242/jcs.130195
- Hahn, M., Dambacher, S., Dulev, S., Kuznetsova, A. Y., Eck, S., Worz, S., . . . Schotta, G. (2013). Suv4-20h2 mediates chromatin compaction and is important for cohesin recruitment to heterochromatin. *Genes Dev*, 27(8), 859-872. doi: 10.1101/gad.210377.112

- Heidinger-Pauli, J. M., Unal, E., & Koshland, D. (2009). Distinct targets of the Eco1 acetyltransferase modulate cohesion in S-phase and in response to DNA damage. *Mol Cell*, 34(3), 311-321. doi: 10.1016/j.molcel.2009.04.008
- Hirano, M., Anderson, D. E., Erickson, H. P., & Hirano, T. (2001). Bimodal activation of SMC ATPase by intra- and inter-molecular interactions. *EMBO J*, 20(12), 3238-3250. doi: 10.1093/emboj/20.12.3238
- Hirano, T. (2006). At the heart of the chromosome: SMC proteins in action. *Nat Rev Mol Cell Biol*, 7(5), 311-322. doi: 10.1038/nrm1909
- Hirano, T. (2015). Chromosome Dynamics during Mitosis. *Cold Spring Harb Perspect Biol*, 7(6). doi: 10.1101/cshperspect.a015792
- Hu, Y., & Parvin, J. D. (2014). Small ubiquitin-like modifier (SUMO) isoforms and conjugation-independent function in DNA double-strand break repair pathways. *J Biol Chem*, 289(31), 21289-21295. doi: 10.1074/jbc.C114.582122
- Irmisch, A., Ampatzidou, E., Mizuno, K., O'Connell, M. J., & Murray, J. M. (2009). Smc5/6 maintains stalled replication forks in a recombination-competent conformation. *EMBO J*, 28(2), 144-155. doi: 10.1038/emboj.2008.273
- Ivanov, D., Schleiffer, A., Eisenhaber, F., Mechtler, K., Haering, C. H., & Nasmyth, K. (2002). Eco1 is a novel acetyltransferase that can acetylate proteins involved in cohesion. *Curr Biol*, 12(4), 323-328.
- Jeppsson, K., Kanno, T., Shirahige, K., & Sjogren, C. (2014). The maintenance of chromosome structure: positioning and functioning of SMC complexes. *Nat Rev Mol Cell Biol*, 15(9), 601-614. doi: 10.1038/nrm3857
- Kegel, A., & Sjogren, C. (2010). The Smc5/6 complex: more than repair? *Cold Spring Harb Symp Quant Biol*, 75, 179-187. doi: 10.1101/sqb.2010.75.047
- Li, X., & Heyer, W. D. (2008). Homologous recombination in DNA repair and DNA damage tolerance. *Cell Res*, 18(1), 99-113. doi: 10.1038/cr.2008.1
- Lindroos, H. B., Strom, L., Itoh, T., Katou, Y., Shirahige, K., & Sjogren, C. (2006). Chromosomal association of the Smc5/6 complex reveals that it functions in differently regulated pathways. *Mol Cell*, 22(6), 755-767. doi: 10.1016/j.molcel.2006.05.014
- Liu, J., & Krantz, I. D. (2009). Cornelia de Lange syndrome, cohesin, and beyond. *Clin Genet*, 76(4), 303-314. doi: 10.1111/j.1399-0004.2009.01271.x
- Liu, Q., Guntuku, S., Cui, X. S., Matsuoka, S., Cortez, D., Tamai, K., . . . Elledge, S. J. (2000). Chk1 is an essential kinase that is regulated by Atr and required for the G(2)/M DNA damage checkpoint. *Genes Dev*, 14(12), 1448-1459.
- McDonald, W. H., Pavlova, Y., Yates, J. R., 3rd, & Boddy, M. N. (2003). Novel essential DNA repair proteins Nse1 and Nse2 are subunits of the fission yeast Smc5-Smc6 complex. *J Biol Chem*, 278(46), 45460-45467. doi: 10.1074/jbc.M308828200
- Miyabe, I., Morishita, T., Hishida, T., Yonei, S., & Shinagawa, H. (2006). Rhp51-dependent recombination intermediates that do not generate checkpoint signal are accumulated in *Schizosaccharomyces pombe* rad60 and smc5/6 mutants after release from replication arrest. *Mol Cell Biol*, 26(1), 343-353. doi: 10.1128/mcb.26.1.343-353.2006
- Muramatsu, D., Singh, P. B., Kimura, H., Tachibana, M., & Shinkai, Y. (2013). Pericentric heterochromatin generated by HP1 protein interaction-defective histone methyltransferase Suv39h1. *J Biol Chem*, 288(35), 25285-25296. doi: 10.1074/jbc.M113.470724
- Murray, J. M., & Carr, A. M. (2008). Smc5/6: a link between DNA repair and unidirectional replication? *Nat Rev Mol Cell Biol*, 9(2), 177-182. doi: 10.1038/nrm2309
- Nagasaka, K., & Hirota, T. (2015). Clarifying the role of condensin in shaping chromosomes. *Nat Cell Biol*, 17(6), 711-713. doi: 10.1038/ncb3183
- Nasmyth, K. (2011). Cohesin: a catenase with separate entry and exit gates? *Nat Cell Biol*, 13(10), 1170-1177. doi: 10.1038/ncb2349
- Noel, J. F., & Wellinger, R. J. (2011). The Smc5/6 complex and the difficulties cutting the ties of twin sisters. *Aging (Albany NY)*, 3(3), 186-188.
- Ohouo, P. Y., & Smolka, M. B. (2011). A touching moment for Smc5/6: from ssDNA binding to repair. *Cell Cycle*, 10(8), 1190-1191.
- Ou, Y. H., Chung, P. H., Sun, T. P., & Shieh, S. Y. (2005). p53 C-terminal phosphorylation by CHK1 and CHK2 participates in the regulation of DNA-damage-induced C-terminal acetylation. *Mol Biol Cell*, 16(4), 1684-1695. doi: 10.1091/mbc.E04-08-0689

- Ouyang, K. J., Woo, L. L., Zhu, J., Huo, D., Matunis, M. J., & Ellis, N. A. (2009). SUMO modification regulates BLM and RAD51 interaction at damaged replication forks. *PLoS Biol*, 7(12), e1000252. doi: 10.1371/journal.pbio.1000252
- Payne, F., Colnaghi, R., Rocha, N., Seth, A., Harris, J., Carpenter, G., . . . Semple, R. (2014). Hypomorphism in human NSMCE2 linked to primordial dwarfism and insulin resistance. *J Clin Invest*, 124(9), 4028-4038. doi: 10.1172/jci73264
- Payne, Felicity, Colnaghi, Rita, Rocha, Nuno, Seth, Asha, Harris, Julie, Carpenter, Gillian, . . . Saudek, Vladimir. (2014). Hypomorphism for human NSMCE2/MMS21 causes primordial dwarfism and insulin resistance.
- Pebernard, S., Schaffer, L., Campbell, D., Head, S. R., & Boddy, M. N. (2008). Localization of Smc5/6 to centromeres and telomeres requires heterochromatin and SUMO, respectively. *EMBO J*, 27(22), 3011-3023. doi: 10.1038/emboj.2008.220
- Peng, J. C., & Karpen, G. H. (2008). Epigenetic regulation of heterochromatic DNA stability. *Curr Opin Genet Dev*, 18(2), 204-211. doi: 10.1016/j.gde.2008.01.021
- Petermann, E., Orta, M. L., Issaeva, N., Schultz, N., & Helleday, T. (2010). Hydroxyurea-stalled replication forks become progressively inactivated and require two different RAD51-mediated pathways for restart and repair. *Mol Cell*, 37(4), 492-502. doi: 10.1016/j.molcel.2010.01.021
- Pommier, Y., Leo, E., Zhang, H., & Marchand, C. (2010). DNA topoisomerases and their poisoning by anticancer and antibacterial drugs. *Chem Biol*, 17(5), 421-433. doi: 10.1016/j.chembiol.2010.04.012
- Potts, P. R. (2009). The Yin and Yang of the MMS21-SMC5/6 SUMO ligase complex in homologous recombination. *DNA Repair (Amst)*, 8(4), 499-506. doi: 10.1016/j.dnarep.2009.01.009
- Potts, P. R., Porteus, M. H., & Yu, H. (2006). Human SMC5/6 complex promotes sister chromatid homologous recombination by recruiting the SMC1/3 cohesin complex to double-strand breaks. *EMBO J*, 25(14), 3377-3388. doi: 10.1038/sj.emboj.7601218
- Potts, P. R., & Yu, H. (2005). Human MMS21/NSE2 is a SUMO ligase required for DNA repair. *Mol Cell Biol*, 25(16), 7021-7032. doi: 10.1128/MCB.25.16.7021-7032.2005
- Rai, R., Varma, S. P., Shinde, N., Ghosh, S., Kumaran, S. P., Skariah, G., & Laloraya, S. (2011). Small ubiquitin-related modifier ligase activity of Mms21 is required for maintenance of chromosome integrity during the unperturbed mitotic cell division cycle in *Saccharomyces cerevisiae*. *J Biol Chem*, 286(16), 14516-14530. doi: 10.1074/jbc.M110.157149
- Rolef Ben-Shahar, T., Heeger, S., Lehane, C., East, P., Flynn, H., Skehel, M., & Uhlmann, F. (2008). Eco1-dependent cohesin acetylation during establishment of sister chromatid cohesion. *Science*, 321(5888), 563-566. doi: 10.1126/science.1157774
- Roy, M. A., & D'Amours, D. (2011). DNA-binding properties of Smc6, a core component of the Smc5-6 DNA repair complex. *Biochem Biophys Res Commun*, 416(1-2), 80-85. doi: 10.1016/j.bbrc.2011.10.149
- Roy, M. A., Siddiqui, N., & D'Amours, D. (2011). Dynamic and selective DNA-binding activity of Smc5, a core component of the Smc5-Smc6 complex. *Cell Cycle*, 10(4), 690-700.
- Saleh-Gohari, N., Bryant, H. E., Schultz, N., Parker, K. M., Cassel, T. N., & Helleday, T. (2005). Spontaneous homologous recombination is induced by collapsed replication forks that are caused by endogenous DNA single-strand breaks. *Mol Cell Biol*, 25(16), 7158-7169. doi: 10.1128/MCB.25.16.7158-7169.2005
- Sambrook, J., & Russell, D. W. (2006). SDS-Polyacrylamide Gel Electrophoresis of Proteins. *CSH Protoc*, 2006(4). doi: 10.1101/pdb.prot4540
- Shintomi, K., & Hirano, T. (2011). The relative ratio of condensin I to II determines chromosome shapes. *Genes Dev*, 25(14), 1464-1469. doi: 10.1101/gad.2060311
- Smith, J., Tho, L. M., Xu, N., & Gillespie, D. A. (2010). The ATM-Chk2 and ATR-Chk1 pathways in DNA damage signaling and cancer. *Adv Cancer Res*, 108, 73-112. doi: 10.1016/b978-0-12-380888-2.00003-0
- Stephan, A. K., Kliszczak, M., Dodson, H., Cooley, C., & Morrison, C. G. (2011). Roles of vertebrate Smc5 in sister chromatid cohesion and homologous recombinational repair. *Mol Cell Biol*, 31(7), 1369-1381. doi: 10.1128/MCB.00786-10
- Stephan, A. K., Kliszczak, M., & Morrison, C. G. (2011). The Nse2/Mms21 SUMO ligase of the Smc5/6 complex in the maintenance of genome stability. *FEBS Lett*, 585(18), 2907-2913. doi: 10.1016/j.febslet.2011.04.067
- Stevens, K. N., Wang, X., Fredericksen, Z., Pankratz, V. S., Cerhan, J., Vachon, C. M., . . . Couch, F. J. (2011). Evaluation of associations between common variation in mitotic regulatory pathways and risk of overall and high grade breast cancer. *Breast Cancer Res Treat*, 129(2), 617-622. doi: 10.1007/s10549-011-1587-y

- Strom, L., Karlsson, C., Lindroos, H. B., Wedahl, S., Katou, Y., Shirahige, K., & Sjogren, C. (2007). Postreplicative formation of cohesion is required for repair and induced by a single DNA break. *Science*, 317(5835), 242-245. doi: 10.1126/science.1140649
- Tapia-Alveal, Claudia, Outwin, Emily A., Trempolec, Natalia, Dziadkowiec, Dorota, Murray, Johanne M., & O'Connell, Matthew J. (2014). SMC complexes and topoisomerase II work together so that sister chromatids can work apart. *Cell Cycle*, 9(11), 2065-2070. doi: 10.4161/cc.9.11.11734
- Taylor, W. R., Agarwal, M. L., Agarwal, A., Stacey, D. W., & Stark, G. R. (1999). p53 inhibits entry into mitosis when DNA synthesis is blocked. *Oncogene*, 18(2), 283-295. doi: 10.1038/sj.onc.1202516
- Todaro, G. J., & Green, H. (1963). Quantitative studies of the growth of mouse embryo cells in culture and their development into established lines. *J Cell Biol*, 17, 299-313.
- Torres-Rosell, J., De Piccoli, G., Cordon-Preciado, V., Farmer, S., Jarmuz, A., Machin, F., . . . Aragon, L. (2007). Anaphase onset before complete DNA replication with intact checkpoint responses. *Science*, 315(5817), 1411-1415. doi: 10.1126/science.1134025
- Torres-Rosell, J., Machin, F., Farmer, S., Jarmuz, A., Eydmann, T., Dalgaard, J. Z., & Aragon, L. (2005). SMC5 and SMC6 genes are required for the segregation of repetitive chromosome regions. *Nat Cell Biol*, 7(4), 412-419. doi: 10.1038/ncb1239
- Torres-Rosell, J., Sunjevaric, I., De Piccoli, G., Sacher, M., Eckert-Boulet, N., Reid, R., . . . Lisby, M. (2007). The Smc5-Smc6 complex and SUMO modification of Rad52 regulates recombinational repair at the ribosomal gene locus. *Nat Cell Biol*, 9(8), 923-931. doi: 10.1038/ncb1619
- Unal, E., Heidinger-Pauli, J. M., & Koshland, D. (2007). DNA double-strand breaks trigger genome-wide sister-chromatid cohesion through Eco1 (Ctf7). *Science*, 317(5835), 245-248. doi: 10.1126/science.1140637
- van Maanen, J. M., Retel, J., de Vries, J., & Pinedo, H. M. (1988). Mechanism of action of antitumor drug etoposide: a review. *J Natl Cancer Inst*, 80(19), 1526-1533.
- Vega, H., Trainer, A. H., Gordillo, M., Crosier, M., Kayserili, H., Skovby, F., . . . Jabs, E. W. (2010). Phenotypic variability in 49 cases of ESCO2 mutations, including novel missense and codon deletion in the acetyltransferase domain, correlates with ESCO2 expression and establishes the clinical criteria for Roberts syndrome. *J Med Genet*, 47(1), 30-37. doi: 10.1136/jmg.2009.068395
- Verkade, H. M., Bugg, S. J., Lindsay, H. D., Carr, A. M., & O'Connell, M. J. (1999). Rad18 is required for DNA repair and checkpoint responses in fission yeast. *Mol Biol Cell*, 10(9), 2905-2918.
- Verver, D. E., van Pelt, A. M., Repping, S., & Hamer, G. (2013). Role for rodent Smc6 in pericentromeric heterochromatin domains during spermatogonial differentiation and meiosis. *Cell Death Dis*, 4, e749. doi: 10.1038/cddis.2013.269
- W. Wilson, Laurence O., & M, Aude. (2013). Condensins, Chromatin Remodeling and Gene Transcription. doi: 10.5772/55732
- Wu, N., Kong, X., Ji, Z., Zeng, W., Potts, P. R., Yokomori, K., & Yu, H. (2012). Scc1 sumoylation by Mms21 promotes sister chromatid recombination through counteracting Wapl. *Genes Dev*, 26(13), 1473-1485. doi: 10.1101/gad.193615.112
- Wu, N., & Yu, H. (2012). The Smc complexes in DNA damage response. *Cell Biosci*, 2, 5. doi: 10.1186/2045-3701-2-5

HIMAJA (HIMA) GADDIPATI

hgaddip1@jhu.edu (719) 351-9547

EDUCATION

Johns Hopkins University Bloomberg School of Public Health **2015**
Master of Science--Biochemistry and Molecular Biology
Adolescent Health Public Health Certificate

University of California-Los Angeles **2012**
Bachelor of Science--Neuroscience

RESEARCH EXPERIENCE

University of Colorado, Denver-Anschutz Medical Campus, Department of Psychiatry (October 2012-August 2013)

Professional Research Assistant—Magnetoencephalography Lab

Supervisor: Dr. Don Rojas

- Recruited and served as a liaison for children and families afflicted with autism spectrum disorder (ASD).
- Recruited and guided child subjects with early-onset psychosis through structured clinical interviews and psychological testing.
- Managed, conducted, and internally audited the lab's MEG recordings.
- Assisted in identifying preoperative epileptic candidates by performing EEG recordings and localizing aberrant spike activity onto a structural MRI.
- Designed and implemented a new procedural protocol for EEG/MEG recordings to make the process smoother for patients.
- Analyzed imaging data to identify structural differences between first degree relatives of children with ASD and control subjects.

Colorado Children's Hospital, Department of Psychiatry, Denver, CO (May 2012-August 2012)

Intern

Supervisor: Dr. Cindy Buchanan and Dr. Harrison Levine

- Evaluated the effectiveness of the Strengthening Alliances with Families team (SAFteam), a consultation service for complex pediatric care that sought to improve communication between patients and medical staff, educate families on recovery routines post discharge, and ensure proper care transition between multidisciplinary providers.
- Assisted Dr. Levine in implementing a quality improvement program for ASD children that would alleviate behavior complications post medical procedures.
- Participated in psychology consults.
- Contributed to a chapter about the harmful effects of relocating post-lung transplantation in Dr. Buchanan's recently published book: "Psychosocial Aspects: Transition to Local Care and Scheduled Follow-up."

UCLA, Department of Psychiatry, Los Angeles, CA (September 2008-June 2012)

Student Researcher

Supervisor: Dr. Teena Moody and Dr. Susan Bookheimer

- Analyzed fMRI data that sought to identify the impact of internet training on working memory in older adults. Presented results at Society for Neuroscience 2009 and 2010, and the UCLA Annual Research Conference on Ageing.
- Conducted MRI scans at the UCLA Ahmanson-Lovelace Brain Mapping center.
- Intermittently designed and coded cognitive tasks for fMRI studies, including Stroop and Go-No-Go tasks.

Army Research Laboratory, Aberdeen, MD (June 2010-August 2010)

Intern

Supervisor: Dr. Shashi Karna

- Investigated the viability of four different EEG systems (Quasar, ABM, BioSemi, and eMotiv) via an error related potential cognitive task (ErrP). Goal was to deduce which system was best for measuring soldier performance.
- Coded the ErrP task and obtained preliminary data from each system.

UCLA Undergraduate Research Consortium in Functional Genomics, Los Angeles, CA (January 2009-March 2009)

Student Researcher

Supervisor: John Olson

- Dissected the brain and eye discs of *Drosophila melanogaster* (fruit fly) in order to characterize gene expression correlated with tissue development.
- Analyzed the expression of ten different genes and wrote a research paper.

POSTERS

Moody, T.D., Gaddipati, H., Small, G.W., Bookheimer, S.Y. (2009). Neural activation patterns in older adults following Internet training. Society for Neuroscience Abstracts,35.

Gaddipati, H., Moody, T.D., Hegarty, C., Shirinyan,D., Small, G.W., Bookheimer, S.Y. (2010) Internet Training Alters Neural Circuitry in Older Adults. UCLA Science Poster Day Abstracts,11.

Gaddipati, H., Moody, T.D., Hegarty, C., Shirinyan,D., Small, G.W., Bookheimer, S.Y. (2010) Internet Training Alters Neural Circuitry in Older Adults. UCLA Annual Research Conference on Aging,21.

Gaddipati, H., Moody, T.D., Shirinyan, D., Small, G .W., Bookheimer, S.Y. (2010) Internet Training Alters Neural Circuitry in Older Adults. Society for Neuroscience Abstracts, 54.

Gaddipati, H, Buchanan, C, Reese, J, Levine, H. (2012) The Effect of Strengthening Alliances with Families Team (SAFTeam) Consultations on Secondary Stress Symptoms in Healthcare Providers while Managing Difficult Patients. PREP poster session.